Snowfall Event Analysis at a Remote Northern Alpine Icefield

by

Eric Courtin
B.Sc., University of Victoria, 2010

A Thesis Submitted in Partial Fulfillment
of the Requirements for the Degree of

MASTER OF SCIENCE

in the Department of Geography

Snowfall Event Analysis at a Remote Northern Alpine Icefield

by

Eric Courtin
B.Sc., University of Victoria, 2010

Supervisory Committee

Dr. David E. Atkinson, (Department of Geography, University of Victoria)
Co-Supervisor

Michael Demuth, P. Eng, P.Geo (Geological Survey of Canada)
Co-Supervisor

Abstract

Data are presented from an automatic weather station on the Brintnell-Bologna Icefield that operated from August 2014 to August 2016 in Nahanni National Park Reserve. This location is notable for being the northernmost mass balance alpine study location of the federal government's glaciology program (NRCan/GSC). The link between atmospheric forcing at the synoptic scale and response at the glacier surface has been shown to be strongly dependent on continentality and latitude. In this region, however, many aspects of the physical processes controlling the interaction between atmospheric forcing and snowpack response are virtually unknown, especially at the daily to hourly timescale.

The character of snowfalls during the accumulation seasons for this icefield are investigated using high resolution time series from two acoustic snow depth sensors and other relevant meteorological parameters. It is found that the most drastic changes in snow depth occur from infrequent large snowfalls. Using an adaption of an Environment Canada snow depth algorithm, snowfall events are identified and their timing is quantified based on a system of thresholds, running averages and ratios between the snow depth sensors. Synoptic conditions are examined using meteorological reanalysis data and trajectory analysis to determine the moisture origin and pathway.

Table of Contents

List of Tables

List of Figures

Acknowledgments

First and foremost, I thank David Atkinson, my supervisor, for the opportunity to be a part of this project and through it pursue alpine climate research. His patience and encouragement gave me the time and inspiration to develop a fulfilling research question. I could not have completed this thesis while balancing family and career commitments without his unwavering support and for that I am much indebted.

I thank Mike Demuth, my co-supervisor, for generous allowances of time and resources to install meteorological stations during mass balance field campaigns. His guidance and mentorship throughout my research was invaluable.

I thank Campbell Scientific Canada, in particular Claude Labine and Carl DeLeeuw, for their longstanding support.

I thank Faron Anslow, my external committee member, for feedback that greatly improved this thesis.

I acknowledge the following organizations and people that provided support either directly or indirectly to this project, without whom it would not have been possible: The University of Victoria, the Geological Survey of Canada, The University of Saskatchewan, May Guan, Steve Bertollo, the National Sciences and Engineering Council, Natural Resources Canada-Polar Continental Shelf Project, the Nahanni National Park Reserve and Parks Canada, and the North America Tungsten Corporation.

A special thank you to John Pomeroy and the University of Saskatchewan's Coldwater lab for allowing the time and flexibility in a busy field work schedule for me to complete my graduate studies.

And a heartfelt thank you to Lauren for putting up with all of this!

1. Motivation and Project History

Meteorological stations are generally installed for meteorological forecasting, and those forecasts are most useful for population centres, which in Canada are predominantly in the south and almost exclusively at low altitude relative to surrounding topography. High-altitude areas show a great variety of meteorological phenomena due to elevation and topography and in turn themselves modify climate by their presence (Barry, 1992). Despite the physical separation of rugged and remote areas from society, these areas affect us in many ways, for example they provide water supplies from melting glaciers and snowpacks, present natural hazards, and control ecological systems (Moore et al, 2009)

Through a partnership between the University of Victoria (UVic), the Geological Survey of Canada (GSC), the University of Saskatchewan (USask), and the assistance of many other people and agencies, the opportunity came about to install a weather station directly on a remote icefield. This weather station had a comprehensive suite of high quality instruments, with satellite telemetry offering near real-time data.

The station operated almost exactly as planned for two full seasons, surviving a toppling over once at the end of the first season (2014-2015, hereafter S1) and was decommissioned after toppling at the end of the second season (2015-2016, hereafter S2). This can still be considered a success: installing equipment on ice is difficult at the best of times, as even keeping a single tripod with a bare minimum of equipment running can be challenging.

The meteorological instruments from this station are of a high standard of quality, and the data offer an unprecedented look into the weather and climate of a high latitude and high altitude area that is poorly understood. Although meteorological monitoring on and in the vicinity of glaciers is not new, stations of this caliber on glaciers are rare even in easily accessed locations. This data legacy, together with ongoing glaciological monitoring by the GSC and hydrometeorological monitoring by USask will offer numerous research opportunities on any number of meteorological, climatological, glaciological, and hydrological studies.

This thesis is intended to serve as a foundation for the research of others, inspiring continued investigating of the links between climate, weather, and ice in this place.

2. Introduction

Hydrometeorological and geophysical research work in alpine areas serves various purposes. Much of Western Canada's mountain ranges possess glacierized features that serve as hydrological storage for the watersheds of the continental interior (Jansson et al, 2003). Cryological features, especially smaller icefields and glaciers, are sensitive to a changing climate and serve as useful climatic monitors (Vaughan et al, 2013). Temperate glaciers are important sources of water in Western Canada (Demuth and Pietroniro, 2003). Glacier melt provides water essential to healthy waterways, as this flow increases during hot, dry years to counter the lower flow (Fountain and Tangborn, 1985). Even more importantly, the glacierized high alpine areas are where extensive snowpacks exist and as such provide most of the surface water for the surrounding low areas for the rest of the year. Operationally, hazard prediction in relation to snow avalanches, mountain aviation, and search and rescue work benefit from an improved understanding of weather processes and snowpack response in alpine regions. These sorts of problems require analyses that consider multiple spatial scales.

Glacier change in area and mass is directly linked to climate forcing on multiple spatial and temporal scales (Dyurgerov and Meier, 1999). Each year the gain or loss depends on the mass balance which is the sum of the winter balance (accumulation season) and summer balance (ablation season) (Benn and Evans, 2014). Winter balance is primarily dependent on precipitation; for the study location it can be assumed to fall exclusively as snow due to latitude and altitude except in summer. The seasonal snowpack is built up by individual precipitation events, which are characterized by their number, duration, and intensity. In turn these events depend on the characteristics of the airmass bringing precipitation, and are shaped by the synoptic conditions controlling the movement of this airmass. Local conditions such as interactions of wind with topography will cause modifications and transport falling and previously deposited snow. Layers in the snow are formed at deposition and over time. For continental sites, large temperature variability, densification due to wind, and lack of melt and water content foster a highly variable snowpack. These can persist due to reduced seasonal metamorphism unlike for example a maritime snowpack which will see significant changes due to temperature equilibrium and melt/freeze processes.

A standard framework for meteorological monitoring is the automated weather station (AWS). A typical station is composed of electronic sensors that record parameters such as snow depth, temperature, humidity, wind speed and direction, etc. and save data for later download or transmission through telemetry. The most common snow surface height monitor is the acoustic snow depth sensor, from which snowfalls, densification, and erosion or melt can be inferred. In alpine areas, a large, unobstructed glacier is an ideal location to monitor snowfall, as a representative measurement can be made for a large area around it (compared to the surrounding topography). This is assuming the location is carefully chosen, away from features interrupting the surface smoothness such as crevasses, moulins, dirt cones, nearby rocks or vegetation. Glaciers also provide a uniformly cold surface.

The glacierized area for this study is the Brintnell-Bologna Icefield (BBI) in Nahanni National Park Reserve (NNPR), notable for being being the northernmost mass balance study location of the Geological Survey of Canada's glaciology program in Western Canada (Demuth et al, 2014). This area is far from the large icefields found in the Saint Elias Mountains to the west or in the Canadian Rocky Mountains and Interior Ranges to the south, that have benefitted from long term glaciological studies and climate studies . The BBI therefore offers an unparalleled opportunity: an extremely remote area can be instrumented with good logistical support, with no precedent in nearby meteorological data except for that associated with several years of glaciological mass balance and geophysical measurements initiated in 2006 (Demuth, personal communication).

Little climatological research has been completed near the Brintnell-Bologna Icefield, with the exception of that associated with hydrological work (Anderson, 2017). A small body of work exists for the Saint Elias Mountains due to having some of the most extensive glaciation, highest peaks, and extreme precipitation found in North America. Mount Logan in particular has had extensive ice coring and hence a wealth of climatological research (e.g. Holdsworth et al, 2003, Fisher et al, 2004, Zdanowicz et al, 2014). The mechanisms of precipitation, however, in this complex area are still poorly understood, with few studies examining possible links between snowfall accumulation and climatology (e.g. Marcus and Ragle, 1970; Rupper et al, 2004). Research here and in other glacierized areas affected by coastal conditions and maritime air masses only seem

to generate more questions than answers. There are seemingly poor links between precipitation and climate indices in this region (Bitz and Batisti, 1999) and between precipitation of nearby high and low altitude sites (Marcus and Ragle, 1970). In a study of six glaciers spanning from Alaska to Washington states and from coastal British Columbia to the Rocky Mountains in Alberta, Bitz and Batisti (1999) found varying relationships between mass balance and climatological variables that appear to be based on continentality and latitude. The Alaskan maritime Wolverine glacier's winter balance (annual balance) was negatively correlated with the winter balance (annual balance) of the southern glaciers on an interannual basis. However, unlike the southern glaciers, the Wolverine glacier showed higher winter mass balance in years with less storminess; the anomalies causing this induce advection of warm moist air and favour orographic lifting. Hodge et al (1998) point out that Wolverine mass balance has very little coherence with the continental Gulkana glacier 350 km away, compared to several similar climate and mass balance linkages between Wolverine and the South Cascade glacier in Washington which is over 2000 km away. Gulkana's continentality is postulated to be due not only to its distance from the ocean but also by the presence of large coastal mountain ranges. While coastal glaciers are influenced by small-scale circulation patterns, glaciers further inland are likely only influenced by large-scale circulations (Yarnal, 1984).

Many studies have examined the links between synoptic meteorology over the Pacific Ocean and precipitation events on the west coast and interior of North America (e.g. Moore and McKendry, 1996; Cayan, 1996). The primary synoptic feature is a strong low-pressure system in the Gulf of Alaska near the Aleutian islands. The position and strength of this system over the course of several seasons can be linked to the frequency of storms along common tracks (Mesquita et al, 2010; Rodionov et al, 2007). Commonly, "typing" can be done where typical conditions are grouped when a large enough sample size allows. This has been done for example on; spring snowpacks using 500 mb synoptic conditions in the United States Rockies (Changnon et al, 1993), comparison of snowfall event frequency from various circulation patterns between western slope and eastern slope Canadian Rocky Mountain glaciers (Sinclair and Marshall, 2009), and relating British Columbia surface weather to large scale atmospheric variability through synoptic types determined through principle components analysis (Stahl et al, 2006).

Climate indices have been developed for relevant teleconnections that link meteorological variables such as sea surface temperature, pressure, precipitation etc. in various regions of the Pacific Ocean and over continental North America. There are numerous examples; links between particular indices and particular glaciers (Moore and Demuth, 2001), snow vs non-snow producing synoptic types in relation to the Pacific Decadal Oscillation (Demuth and Keller, 2006), strong/weak index relation to high and low altitude (Moore et al, 2003), tropical vs. north pacific index correlations to glaciers (Hodge et al, 1998), etc. Of particular importance for this study is the well-documented variability of storm tracks due to atmospheric forcing and teleconnections, such as El Nino Southern Oscillation and the Pacific North America pattern (Trenberth and Hurrell, 1994). In the winter, a confluence of air masses in this area can bring very different conditions to nearby areas (Yarnal, 1985). This can lead to a north/south mass balance bifurcation whereby the northern reaches of the cordillera are preferentially nourished in the winter at the expense of the sourthern reaches and vice versa (Walters and Meier, 1989; Demuth et al, 2008). For exceptional precipitation events, case studies with a chronological description of the evolution of the synoptic conditions make for effective presentation (e.g. Lackmann and Gyakum, 1997; Lackmann et al, 1999). Similar data sources to the "typing" studies are used; reanalysis, AWS data, model simulations, and trajectory analysis. Together these form a standard methodology for many studies examining the origin of precipitation (e.g. Shea and Marshall, 2007).

The high quality and high altitude long term snowfall data sets in the Western United States has led to many studies of snowpack and SWE (e.g. Serreze et al, 2001) in well-defined maritime, intermountain, and continental climate zones (Armstrong and Armstrong, 1987). Several studies have examined the link between synoptic scale storms and extreme snowfall (Rutz et al, 2014; Swales et al, 2016) and compared them mostly on a seasonal scale. Birkeland and Mock (1996) discovered that the extreme snowfall events (>33 cm in a day) at their intermountain site was due to synoptic northwesterly flow and determined that this was due to topographical controls by other mountain ranges en-route. This result was determined by studying individual events and contradicted results from similar studies done on the seasonal timescale. Studies of individual snowfall events measured at various locations at a maritime mountain ski resort showed a change in relative accumulations across the mountain due to storm track fluctuations (Burak and

Davis, 1998). The link between synoptic weather and heavy precipitation requires study of moisture pathways, such as those done for the Intermountain West of the United States by Alexander et al (2015) and Swales et al (2016). As it concerns Western Canada's alpine regions, there is a paucity of research that consider intra-event or inter-event extreme snowfall comparisons in combination with synoptic and trajectory analysis in Canada.

Research Questions, Goals, and Limitations

The research in this thesis was spurred by several unexpectedly large snowfalls early in the first accumulation season after the installation of the BBI AWS. Given the location of the icefield (well inland), the mechanisms that could lead to a large snowfall are not obvious. It could be expected that a continental climate would manifest shorter, more frequent snowfalls rather than large, infrequent snowfalls typical of a maritime climate (e.g. Lute and Abatzoglou, 2014). It was decided to study this by integrating moisture source, transport overland and the controlling atmospheric conditions, and, in particular, focus on the timing of individual accumulations, given the opportunity afforded by the high resolution of the meteorological data. The research question was, therefore: What are the synoptic and topographical controls of snowfall at this location?

This research question has many important qualities.

1) The focus on snow is appropriate for this glaciological-centric project.
2) The challenge of determining snowfall event timing requires a blend of quantitative analysis, qualitative observation and technical knowledge.
3) A truly geographical approach, using a range of spatial and temporal scales.
4) The opportunity to use high quality in-situ data to ground-truth a study of a poorly understood and instrumented area.

3. Study Area Geography and Climatology

The Brintnell-Bologna Icefield (BBI), situated within the Nahanni National Park Reserve (NNPR), is the only major icefield in the Selwyn and Mackenzie Mountains. These adjacent mountain ranges are located along the Yukon-Northwest Territory boundary. They are located north of, but are not considered a part of, the Northern Rocky Mountains. The BBI is located in the Ragged Range of the Selwyn Mountains (Figures 1 and 2). To the east lies the Canadian Shield with altitudes less than 600 m above sea level (ASL). This region is termed the Barren Lands. Waters from the BBI feed the Liard River complex via the South Nahanni and Liard rivers, and form an important tributary system for the Mackenzie River. To the west, several large mountain ranges and high elevation areas stand between NNPR and the Pacific Ocean, which is the nearest source of moisture (approximately 630 km to the southwest in the Alaska Panhandle). Other sources of summer moisture for this region are the Beaufort Sea to the north (~800-1000 km away); two large lakes, Great Bear Lake and Great Slave Lake to the east (~400-500 km away); and the wetlands of southern Northwest Territories and Nunavut. All of these water bodies, except the Pacific Ocean, are frozen in winter.

Figure 1: Brintnell-Bologna Glacier location in Western Canada

Figure 2: Satellite images of the Brintnell-Bologna study area in the Ragged Range of the Selwyn Mountains, NT.

Interestingly, the southern Beaufort Sea, although completely covered in ice from October until April (Figure 3), is known to have a large effect on the storm activity of the northern Mackenzie River basin, with a significant reduction in storm activity once it freezes over (Hudak and Young, 2002). The Gulf of Mexico cannot be ignored as a potential source of moisture, given its importance to the Canadian prairies. It is known that it can lead to extreme precipitation events in the Mackenzie River Basin (Brimelow and Reuter, 2005). However given that the synoptic conditions favoring this transport are present mostly in the summer, and the extreme distance to the BBI, it appears to be an implausible source.

The elevation of most of southern Yukon, which lies between the ocean and the icefield, is around 600-1200m ASL, with only a few areas reaching 1800m until the coast. Here the Saint Elias Mountains contain large icefield and glacier complexes where elevations are rarely below 2800 meters and include some of the highest peaks in North America, some of them over 5000 meters ASL. Proximity to the coast contributes to the generation of large snowfall amounts here. These ranges form a significant barrier to precipitation.

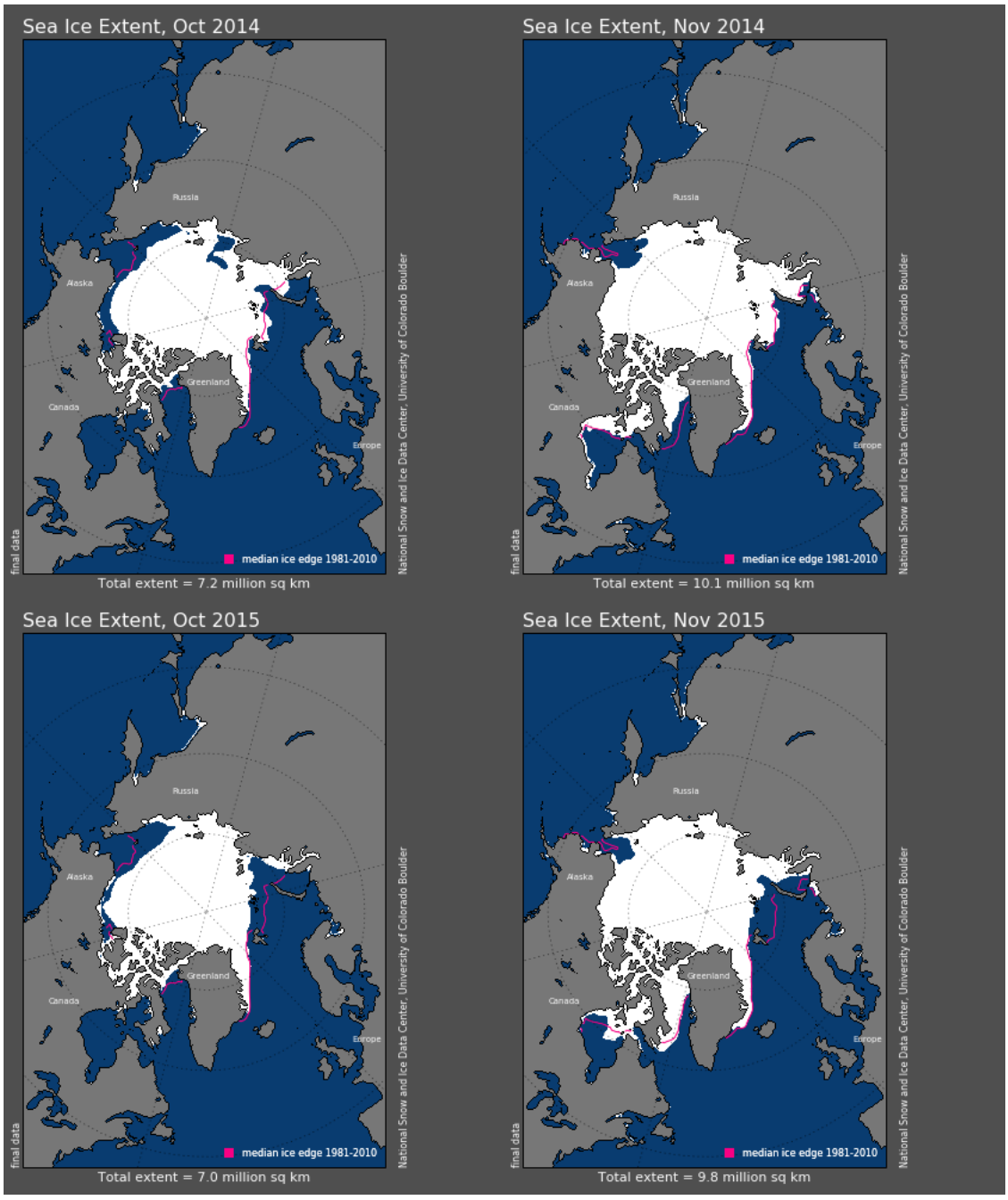

Figure 3: Sea ice extent, October and November 2014 and 2015. (NSIDC, 2018)

The glaciers in NNPR are in retreat, showing a 30% reduction in area between 1982 and 2008 (Demuth et al, 2014). The greatest total reductions were observed for glaciers between 1-10 km^2 due to their large proportion of the total ice in the area. A greater percentage loss was observed for glaciers in the 0.1-1 km^2 size range and many disappeared. In comparison to glacier change in various regions across British Columbia and Alberta from 1985 to 2005 as investigated by Bolch et al (2010), the glaciers of NNPR are typical in their proportion of ice and variation in rate of disappearance across glacier size ranges. Overall, however, their net rate of disappearance is higher than the average of any of the regions studied by Bolch et al. The exception to the disappearance of ice in NNPR was the potential growth of a few very small glaciers that are topographically preserved, which has also been observed in southern areas of the Canadian Cordillera (DeBeer and Sharp, 2009). The BBI is the largest glacier feature in the NNPR, with its 30 km^2 surface representing 15% of the total ice cover in NNPR. BBI is currently in a negative mass balance regime and now has recently lost all of its firn pack (Demuth, personal communication). Elevation varies between 1,770 and 2,450 m ASL The long term equilibrium line altitude (ELA) is at 2,280 m ASL (Demuth et al, 2014).

The AWS is located in the ablation zone of the Bologna Glacier, one of the two main outlet glaciers of the Icefield (Figure 2); the coordinates are 62°06'54.0"N 128°00'26.1"W. The Bologna Glacier's aspect is predominantly northwest. From the southwest counterclockwise to the north are areas of higher elevation up towards the icefield summit region; the weather station is in a bowl with a nunatak to the south (Figure 4), rocky peaks to the north, and the highest elevations of the icefield between the two.

Little research has been conducted in this remote area, and most has focussed on geology, particularly seismic activities, and ecology. Climate information in the literature appears to be limited to a 1983 report from Parks Canada stating that the effects of Arctic and Pacific air masses, topography, and high altitude determine the precipitation and temperature in the park (Spence, 2002), and Halliwell and Catto (2003) state that Pacific Ocean air streams dominate during summer and fall, while Arctic air streams predominate in winter and spring. There are no weather stations currently operating in the immediate area that are suitable for comparison. A current installation is at Rabbit Kettle

Lake, which is approximately 40 km away. Precipitation is not recorded at this location, however. There are also a significant number of missing data as well as potentially questionable data, which would make it unsuitable particularly given the need for the hourly-daily timescale. The University of Saskatchewan station that was on the nearby Nunatak suffered from diurnal power loss and was as such also not used. Environment Canada operated an AWS at the nearby Tungsten mine from 1966 to 1990. While the mine does have a currently operating weather station, the location of the mine in a deep valley does not necessarily make it a good comparison to the likely orographic character of the incoming weather to the region. The station's industrial surroundings also possibly introduce bias for most meteorological variables.

It is worth noting that the NNPR is a very large area (30,050 km^2) and that the study area is close to the western border of the Park Reserve. Beyond the Ragged Range, there are many more subranges (and therefore topographical obstacles) to the east/northeast than to the west.

Figure 4: The Nunatak, with the AWS in the foreground.

4. Data and Methods

4.1 Automatic Weather Station

On August 21st 2014, the installation of an automatic weather station (AWS) was completed on Bologna Glacier in the NNPR (Figure 5). The station included a comprehensive suite of meteorological instruments including two snow depth sensors, three vertical levels of wind, temperature and humidity monitoring, four-component radiation, snow pack temperature, surface radiant temperature, atmospheric pressure, and a snow water equivalent (SWE) sensor. The measurement principle of this SWE sensor is that attenuation by water of gamma radiation from potassium isotopes in organic material can be used to calculate the SWE of the snowpack. No radiation would penetrate the depth of a glacier, so a source of potassium on the ice surface was used. Also installed was a digital camera, installed on the tripod and facing the tower. The field of view was chosen to include the mid-section of the tower and the snow surface around it, the glacier

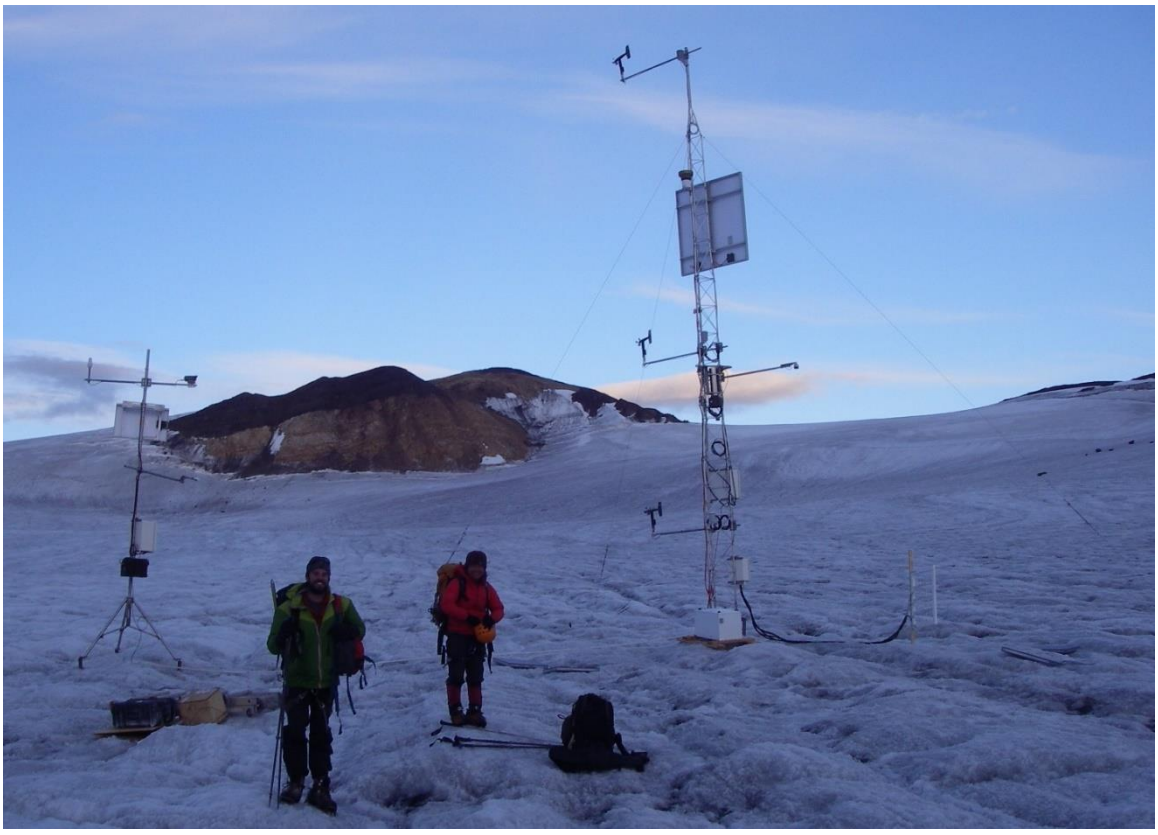

Figure 5: Weather station after original install in August 2014. Photo orientation is due east. Brintnell drainage is beyond the image skyline.

Figure 6: Image of the meteorological tower toppling over in summer 2015, from top to bottom: 08/02, 08/03, 08/04. The camera is located on the tripod which toppled one month prior. The guy wire anchor can be seen coming out in the second picture.

surface and nunatak in the background, and the sky. High resolution hourly images were taken throughout the day and a low resolution picture was taken every day at noon. A satellite telemetry system was used to collect all of the data and one of the daily noon images on a weekly basis. Monitoring of the data and conditions began immediately, including sensor performance and their response to events of note. The station operated without significant interruption until July 18th, 2015. Timely receipt of a satellite image of the tower anchor melting out of the ice (Figure 6) provided information that the tower had fallen so that an appropriate response could be prepared for the next field trip.

Reinstallation of the mostly undamaged tower

on August 20th 2015 provided another year of data, with the station being removed intact on August 4th 2016.

The study of snowfall events was restricted to the accumulation season on the glacier. The dates analyzed are from September 1st 2014 to April 30th 2015 and September 1st 2015 to April 30th 2016. These months were chosen to study accumulation as the measurement of winter mass balance is generally performed at this location in May and the summer mass balance measurements in mid-late August.

4.1.1 Snow

The SR50A sensor manufactured by Campbell Scientific (Canada) Corporation outputs a distance to target measurement using the time of flight of an acoustic pulse which reflects off the snow surface. The measurement is corrected for speed of sound variations as a function of air density using air temperature. For each measurement a data quality indicator aids interpretation. High quality numbers signify a strong signal from a uniform flat surface. Low quality numbers indicate a weaker return signal, which can be caused by blowing snow, an uneven surface, and/or a very low-density snow surface that enables the acoustic pulse to partially penetrate surface snow and reflect off denser snow beneath (Goodison et al, 1988). To avoid errors due to these factors, each single snow depth reading in the data is the median of 11 measurements taken within a few seconds, the recommended practice from the manufacturer (Campbell Scientific (Canada) Corp., 2012). Erroneous readings (i.e. “0” or “NAN” (not a number)) or over range errors are possible and so taking the median is necessary in order not to average those readings. If desired, monitoring for conditions such as blowing snow or penetration of the acoustic pulse through light density snow can be performed through using a signal quality indicator. These techniques improve data fidelity significantly during snowfall events.

Snow depth readings were recorded every 15 minutes to maximize resolution during rapid accumulation events. The sensors were on the ends of cross-arms approximately 2 meters long, and installed 340 and 380 cm off the ice surface. With a field of view of approximately 30 degrees, it was calculated that the sensor would not detect the tower itself but readings could easily be affected by the drift (on the lee side) or scour (on the windward side) caused by the tower’s interruption of the local wind field. For this reason,

the two sensors were installed on opposing sides of the tower to minimize the susceptibility of both sensors to be affected by the same micro-scale feature.

4.1.2 Wind, Temperature, and Relative Humidity

The wind sensors used are integrated propeller and vane R.M. Young 05103-45 Alpine model anemometers. The temperature and relative humidity sensors are Rotronic HC2-S3 sensors in radiation shields. Both of these sensors were installed at each of three heights on the tower: 140 cm, 430 cm, and 915 cm from the base of the tower at ice level as of the installation date. Like most sensors on the station (with the exception of snow depth), these sensors are sampled at 5 second intervals, and hourly and daily averages are compiled and reported in the data table. Maxima and minima for those intervals are also collected, as well as standard deviation for direction. Wind speed and direction was considered to aid in determining what topographical controls there may have been on snowfall events. Temperature and humidity was used to verify passage of moist airmasses.

4.2 Snowfall event algorithm

To identify synoptic controls on major snowfall events, the timing and magnitude of individual events must be quantified. Raw snow depth data derived from sonic depth gauges are not suitable for direct analysis; they are a record not only of snowfall but also of redistribution due to wind, sublimation, densification, and noise in the data. These influences will occur on multiple spatial and temporal scales. Wind will modify the snowpack surface primarily through erosional and depositional mechanisms called “snow bedforms” (Filhol and Sturm, 2015). These occur even on homogeneous flat snowpacks. The most significant snowpack modifications will occur from wind redistribution or preferential melting due to topography or nearby obstacles. On the icefield, the only nearby potential cause of this is the tower itself. For this reason, only relative increases between the sensors should be calculated, not the absolute difference between them. Densification occurs continuously, including during snowfall. This could affect interpretation of when a snowfall event is occurring if for example a light intermittent

snowfall is subject to rapid densification. Finally, small variations between what should be identical measurements are unavoidable due to the electronic nature of the sensor: these errors are manifested as the resolution (0.25 mm) and the accuracy (1 cm).

For a study of snowfall occurrence linked to synoptic scale events, the primary requirement is to precisely measure timing. The start and end time should be well defined to relate the event to synoptic conditions. Breaks in the accumulation must be explainable (i.e. interruption in moisture delivery to the area, high wind speeds causing redistribution). Most algorithms used to analyse snowfall are focused on amount of snow delivered, but the data source and the errors that must be corrected remain the same. Most involve running averages to eliminate noise (Ryan et al. 2008), summing of differences of depths to eliminate densification (Brazenec and Doeksen, 2005), and use of multiple sensors to eliminate spatial variation (Fischer et al. 2011). Some studies over larger temporal scales (i.e. many years of data in study areas with more frequent snowfalls) do not require an algorithm (e.g. Sinclair et al, 2011), however to examine processes within a snowfall event, obtaining accurate timing becomes essential.

The snowfall timing algorithm (hereafter STA) used here incorporates elements of an algorithm as described by Fischer (2011) called “S3-1”. They used three collocated snow depth sensors, a weighing precipitation gauge, and a camera. Weighing gauges have buckets into which precipitation collects and melts, and the weight output corresponds to equivalent of the snow in liquid water. Due to the logistic considerations, use of a weighing precipitation gauge is not possible at sites where the receptacle cannot be regularly emptied and refilled with antifreeze (to prevent freezing) and oil (to prevent evaporation). Gauge topping can also be an issue during high intensity snow accumulation events. While data from the SWE sensor deployed at this AWS would have been an acceptable substitute for a weighing gauge, the data was determined not to be usable. The primary reason is a higher attenuation of the signal than expected after the first few snowfalls led to noise in the data.

The focus of this study is to analyze conditions producing snowfall rather than the characteristics of the snowfall itself. Depth would not be sufficient for a typical snowfall analysis, as SWE depends on density as well, which can vary widely depending on the synoptic conditions that produce it (e.g. Judson and Doeksen, 2000). The S3-1 algorithm is designed to estimate snowfall quantities and therefore is optimized to account for

density. However, for this study, because event timing is the most important parameter, two snow depth sensors alone are largely sufficient for analysis using the STA. In cases where the two sensors are not sufficient to understand what is happening at the snowpack level, the other sensors and the camera can be used to aid interpretation of prevailing meteorological conditions.

Table 1: Algorithm step comparison for this study and Fischer (2011).

Step	S3-1	STA
1	Take measurements from **three** SR50As **and a weighing gauge**	Take measurements from **two** SR50As **11 times and use the median**
2		**Calculate the running average**
3	Verify that at least **two of the three** sensors are recording an increase and verify with weighing gauge	Check that there is an increase in the **average of the two sensors** that is greater than a threshold.
4		Verify that the ratio of the two sensors is within a threshold
5	Compare the current measurement to the placeholder	Compare the current measurement to the placeholder
6	If the difference is greater than MIDST, set new placeholders, **snowfall condition is true**	If current measurement is greater than placeholder, threshold condition is true
7	Calculate ratio between all sensors	If ratio between sensors is less than threshold, ratio condition is true
8	**Various snowfall amounts are calculated depending on number of sensors within the ratio**	If ratio and threshold conditions are true, **snowfall condition is true**
9	If **change in SD is negative**, reset placeholder and snowfall event ends	If **snowdepth is less than placeholder minus threshold**, reset placeholder and snowfall event ends

The possibility of using a signal processing method such as Fourier transforms or wavelet analysis was considered but ultimately rejected, as these are effective in analysing time series with multiple unknown but sinusoidal frequencies superimposed on one another. For a time series of snow depth, most variations in snow depth are not caused by a periodic influence and therefore the applicability of Fourier analysis appears limited. Cumulative summation of consecutive differences is another common way of identifying events and calculating magnitude. First, the difference between two consecutive snow depth measurements is calculated. Each measurement is an average of measurements before and after to create a one-day running average. The measurements from the two traces are then averaged together. While this was proven to be a good way to visualize events, it was, in the end, not needed to bolster or add to what the STA provided.

The individual steps in data processing of S3-1 and STA are similar and the equivalent steps are individually compared in table 1. The order of the steps differs between the two algorithms and so the order shown is that of the STA. The exact steps and order of processing for S3-1 can be verified in Fischer (2011). Differences are in bold, and steps for STA with no equivalent in S3-1 are left blank. For the S3-1 algorithm MISDT refers to “minimum increase in snow depth threshold”.

On a daily to seasonal scale, the snowfalls of interest are distinguishable without analysis or computation. This is due to the discontinuities in rate of change of the snow depth time series before, during and after snowfall events. As such the primary requirement of the STA was to successfully identify all of these intuitively identifiable events. Manual classification of synoptic events offers the advantage of oversight of a trained observer; this lessens the chance of undetected problems or misclassifications by an automated system (Frakes and Yarnal, 1997). The weakness of this decision making is the potential introduction of inconsistency due to subjectivity on the part of the observer. Examination of snowfall event occurrence at the sub-hourly level does not offer the same intuitive clarity in delineation between occurrence and absence of snowfall. This is due to small variations in snowpack depth which can be unrelated to fresh snowfall. This makes an objective process desirable at this scale. The main value of the STA is, therefore, to provide standardization in the processing of start and end determination of snowfall events. Often, the process of developing the STA necessitated iterative changes based on

either empirical evidence of the algorithm performance or a physical basis for the choice of parameters.

The first step of the STA is a running average. This was needed to remove noise due to the accuracy and resolution of the sensors, as well as issues relating to penetration of the snowpack and blowing snow as previously described. A range of running averages were tested to optimize random noise reduction while minimizing the smoothing inherent with running averages. Intervals of 1, 3, and 6 hours were tested, as these were within a range appropriate for synoptic analysis; ultimately 3 hours was chosen. The same 15 minute data resolution as the snow depth time-series was kept, with the 3 hour interval being centered around the corresponding timestamp (1.5 hours of data before and after). Some trace snowfalls on the order of a few cm and lasting a few hours or less will inevitably be reduced or obscured by this processing, with bias increasing with event brevity. However these snowfalls are not important to the analysis, and neither is the small reduction of snowfall magnitude for the larger events given the focus on timing and not quantity. The running average is the biggest difference as compared to the S3-1 algorithm. S3-1 is not lacking for excluding this step, as there are multiple sensors used to detect and filter out insignificant changes

The second step in the processing is the determination of the beginning of snowfall, using the running average data. This was determined to have occurred when the following conditions were met between two successive data points: 1) both sensors individually recorded a positive increase, 2) the comparative increase between the sensors is above a specified ratio and 3) when a threshold of increase is met or exceeded in the difference between the average of the two sensors at the previous timestamp compared to the current one. The first condition ensures that an increase in snow depth is being detected for both sensors, the second that both sensors are recording increases of similar magnitude, as during true snowfall, and the third condition ensures that non-trivial increases do not cause false positives. When the above conditions are true, the snowfall event either begins, or if already ongoing, the current snowdepth is updated to be the current “last maximum”, equivalent of the placeholder in S3-1. The ratio was chosen to be 35%, the same as in S3-1, and the threshold was an empirically chosen value.

The method of ending snowfalls was chosen to be a reduction in average snow depth for a threshold less than the last maximum. Typically during snowfall there is noise due

to the light density snow, which can cause random increases and decreases. In this way, small redistributions do not either prolong the end of an event or cause false negatives by prematurely ending a large-scale event during a small break. The snowpack must have settled to an extent beyond the last identified snowfall interval in order for the event to be considered over. In S3-1, snowfall is considered to have ended when a negative snow depth is identified. This is clearly preferable purely from the perspective of a snowpack analysis, as small changes in densification are important and must be quantified.

The only problem with the algorithm's primary requirement of timing identification appeared to be potential unnecessary extensions of the events. By way of an example, the issue was observed during preliminary testing near the end of an event, with a continuous net increase but with wildly varying individual readings from one sensor. As per the premise of detecting true snowfalls, the successive increases for both sensors must be within a certain ratio. In the case of strong wind during blowing snow, the ratio condition was not true, and therefore the snowfall beginning / continuing condition was not true. Therefore the last maximum was not updated for a substantive amount of snowfall, and the algorithm did not trigger the end of the event until the snow depth dropped below the last maximum, which was well after the event had ended. In practice this was not an issue as it was easily identified by a human observer considering the processes at work. However, for the envisioned use of such an algorithm to automatic application requiring minimal manual input, this physical case will require a modification or additional processing.

4.3 Reanalysis

Reanalyses are datasets of meteorological parameters derived from purpose-run weather forecast models that completely describe the atmosphere system. Available observations such as data from AWS, radiosondes, and remote sensing are assimilated into model runs with a gridded output. This produces regular temporal and spatial resolution for long periods of time (decades) and large areas (continental, global) making them ideal for climatological research. For this study, the reanalysis helps elucidate the link between historical regional meteorological patterns with local weather.

For this study, the North American Regional Reanalysis (Mesinger et al. 2006) was chosen for two reasons. First, this reanalysis product is an "atmospheric and land-surface hydrology dataset" that was designed to have significant improvements over past reanalyses by assimilating precipitation data specifically. A degree of caution is necessary as the input precipitation data is only from rain gauges, and the precipitation rate and accumulation outputs that will be examined are therefore modelled only. However it can be expected that the hydrological focus makes it a suitable option for studying precipitation rate. It is offered in near real-time online, making it an excellent research tool. Second, it possesses the highest spatial resolution available (~32km) of the existing reanalyses for this region, which is important in topographically complex terrain, where large variation in elevation occurs over small horizontal distances. This was also a consideration for performing the back-trajectory work (described below).

Reanalysis products are known to have biases arise from parameterizations and data source inhomogeneities (e.g., Lader 2016). It is to be expected that reanalyses will generally be designed for, and evaluated in, areas with a large population or otherwise of interest to society. NARR is known to replicate continental U.S. precipitation well (Bukovsky and Karoly, 2007) but outside of this area they suggest caution in using the precipitation analysis. As well it should be expected in general that the performance of any reanalysis product at the local scale in Canada's North to be of higher uncertainty; the scarcity of data will cause both less data for input and less opportunity to test output. This may be countered to some extent by spatial resolution increasing with latitude.

4.3.1 Plots

NARR data is provided by NOAA/OAR/ESRL PSD, Boulder, Colorado, USA, from their Web site at https://www.esrl.noaa.gov/psd/. Three main plots are used for analysis from the reanalysis parameters. Columnar (vertically integrated) precipitable water is used to track large-scale moisture transport from the open ocean towards and over the continent. This is the total amount of moisture available for precipitation in a column above the earth's surface. 500 mb geopotential height is used to study low-pressure systems that will force synoptic-scale weather, as well as ridges and troughs shaped by the jetstream. The wind was analysed at 750 mb, found to be the typical altitude of moisture advection in the Canadian Rocky Mountains by Sinclair and Marshall (2009)

and this altitude is used to verify the hysplit trajectories (as opposed to the standard 700 mb height used in upper air analysis). Precipitation variables at higher resolution are considered, however care is taken in their interpretation for the reasons already mentioned. They are primarily used to give insight as to the spatial distribution of precipitation at times when it is snowing on the icefield.

These variables are plotted on two scales. All variables were considered on a large scale, from 30° to 80° Latitude and 180° to 270° degrees Longitude. This encompasses enough of North America and the Northeast pacific for tracking air mass movement. It was useful to view some variables such as 750mb wind on a smaller scale: 56° to 68° Latitude and 212° to 252° degrees Longitude. The 0.3 x 0.3 degree resolution NARR output can be visualized well for this size. These values were chosen such that the study area was centered on the map. Variables are plotted at 3-hourly intervals. Seasonal plots which are composites of particular days of interest are also used.

4.3.2 Hysplit

Hysplit is a trajectory analysis program available online that allows extrapolation of the movement of a parcel of air based on reanalysis data and a digital elevation model (Stein et al, 2015; Rolph et al, 2017). Trajectory analysis allows verification of the interaction of the atmospheric circulation with topography. The reanalysis used for Hysplit runs was NARR and it was run in back-trajectory mode; that is, the ending location and time is set and the trajectory is run back in time.

For regions with multiple moisture sources (i.e. smaller landmasses surrounded by ocean), snowfall characteristics can vary across the region and an isotopic analysis of the snow can be valuable (Sinclair and Marshall, 2009). However, for the BBI, it is certain that the Pacific Ocean is the moisture source for all events in the winter. A time window of 120 hours is chosen to verify the duration of the snowfall event (approximately 1-3 days: Serrreze et al, 2001) but also encompasses moisture transport from across the Northeast Pacific. This is the most likely origin for storm tracks impacting the Northwest coast of North America (Hoskins and Hodges, 2002), with moisture advected from over the ocean due to surface convergence (Trenberth et al, 2003).

Six ending elevations over the BBI are considered: 500, 1000, 1500, 2000, 2500, and 3000 meters above ground level. This corresponds to 2113, 2613, 3113, 3613, 4113, and 4613 meters above sea level, and approximate pressure levels of 780, 740, 690, 650, 610, and 570mb. Multiple ending elevations were used to ascertain the degree to which origins and trajectories are similar, giving evidence of the altitudes of moisture transport. Another reason is that the topography in NARR is smoothed significantly for areas with heterogeneous topography (Hunter, 2016), and so a variety of elevations calculated above the surface were used to account for relative heights above the icefield and absolute heights above sea level. It was decided, however, not to modify ending location horizontally, since the minimum horizontal movement would have to be 0.3 degrees away (the grid size), which, for this study site, would mean significant topographical changes. It is realistic that a trajectory ending in a valley separated from the glacier by several high mountains could follow an entirely different trajectory.

4.4 Summary of world, Northern Hemisphere, and local weather station climate

The following climate normals data for world conditions is from the National Oceanic and Atmospheric Administration of the United States (NOAA, 2016), and for specific Canadian AWS it is from Environment and Climate Change Canada for normal (ECCC, 2016a) and monthly historical station data (ECCC, 2016b).

In 2014-2015, each month was on average the warmest on record for ocean temperatures in the Northern Hemisphere (dating back to 1880) except February (it was the second warmest February on record). For temperatures over land in the northern hemisphere, all months were amongst the ten warmest except one. In 2015-2016, all months supplanted 2014-2015 for warmest ocean temperatures, and all but three months were the warmest on record over land as well.

Monthly data and climate normals for select weather stations in the Yukon, Alaska, British Columbia and Northwest Territories were analysed and compared to data in S1 and S2 from October to April. Every month in every location was warmer than the normal except December in Teslin and February in Faro in S1. Fort Simpson, the only station to the east of the Mackenzie mountains, did not follow this pattern, with several

months cooler than normal. In S2, September was cooler at all stations than normal. November, January, February, and April were all exceptionally warm, with most locations being between 3 and 7 degrees warmer than average.

Precipitation showed more variability between stations. In S1, monthly values ranged from ~ -100% to ~ +140% compared to normal. September and January were significantly wetter, whereas October, November, December and February were significantly drier, again with the exception of Fort Simpson. March and April had more moderate differences, and perhaps reveal a trend of increased coastal and decreased interior precipitation. In S2, the variation per month from the normal was between ~ -80 to ~ 320%. September and October were drier at most stations. A strong decrease in precipitation for every station was observed in December. January, February, and March showed variability with large increases in precipitation being observed at some stations and large decreases at others. April was wetter overall at all stations.

The 2014-15 season marked record mass losses (referring to the "2015" glacier mass balance year) for glaciers in the Pacific Northwest and southwestern Canada, whereas 2015-16 (referring to the "2016" glacier mass balance year) displayed much more modest losses (Demuth and Horne, 2017).

5. Results

5.1 Automatic Weather Station

Data from the University of Victoria AWS was considered from September to April of season 1 (S1) and season 2 (S2) for this study. The primary variables used are snow depth and wind speed and direction. Temperature was also considered to monitor changes in air mass during the events. Other variables were not required for analysis.

5.1.1 Temperature

The temperature data showed an expected regime where the average is higher for the upper sensors (Table 2 and 3) as compared to the sensors closest to the glacier surface. The averages listed are calculated by taking the average of all the hourly averages for the month. The minimum (maximum) is the absolute minimum (maximum) reading recorded for the month.

Table 2. Temperature in °C by sensor and month for 2014-2015

	Sep	Oct	Nov	Dec	Jan	Feb	Mar	Apr
915 cm average	-1.1	-7.0	-11.1	-11.7	-13.0	-14.4	-12.3	-7.7
915 cm minimum	-11.2	-16.1	-27.5	-23.6	-27.7	-38.2	-28.0	-15.6
915 cm maximum	8.2	0.7	4.1	-3.1	-2.5	-1.4	-1.8	2.6
430 cm average	-1.2	-7.1	-11.4	-11.9	-13.2	-14.6	-12.6	-7.9
140 cm average	-1.7	-7.5	-12.5	-12.6	-14.2	-15.6	-13.8	-8.6

Table 3. Temperature in °C by sensor and month for 2015-2016

	Sep	Oct	Nov	Dec	Jan	Feb	Mar	Apr
915 cm average	-3.1	-5.2	-12.3	-14.1	-9.9	-12.0	-10.6	-5.0
915 cm minimum	-15.3	-15.5	-28.2	-27.9	-20.3	-28.6	-18.6	-12.3
915 cm maximum	4.9	4.2	-1.6	-1.7	-2.9	-3.6	0.5	4.8
430 cm average	-3.1	-5.4	-12.5	-14.5	-10.3	-12.3	-10.9	-5.2
140 cm average	-3.3	-5.9	-13.0	-15.7	-11.4	-13.3	-11.6	-5.8

5.1.2 Snow

The total snow accumulation was approximately 1.65 meters for S1. During S2, one of the sensors appears to suffer from an intermittent fault. This could have been due to occasional detection of an obstruction, or degradation of the transducer. However after the first major snowfall event on November 20th, the data appears clean. The snow depth was calculated from the reliable sensor from September 6th to November 20th at 4:00, giving 35 cm. After this date the running average trace from both sensors appears acceptable and measured a total of 1.43 meters. The total from S2 is therefore approximately 1.78 meters. For both seasons, the difference between the two sensors for particular readings was as great as 20 cm or more, however, in general, such large differences were transient and observed on shorter timescales. On average the sensors differed by 11 cm with a standard deviation of 4 cm for S1. When considering the roughness of the surface, this value was considered reasonable (Figure 7).

In the case when recorded measurements were “zero”, the previous good value was chosen to replace it. This allows processing of the data without interruption, and avoids introducing artificial data by, for example, extrapolating between good data. The zeroes could be due to icing or temporary electronic malfunction. Some records were inexplicably missing with no apparent cause (i.e. they could not be explained by typical problematic conditions such as very low temperature, low battery voltage, etc.). When this did occur, the error would sometimes be isolated to one single record or display a pattern, such as the first of the four measurements per hour would be missing for several

hours at a time. However, the occurrence of this problem was sporadic; there were 125 measurements missing in S1 out of 24085. This is symptomatic of a data handling problem; it is possible the datalogger was too “busy” at the time. However other than this almost negligible error, the sensors performed flawlessly.

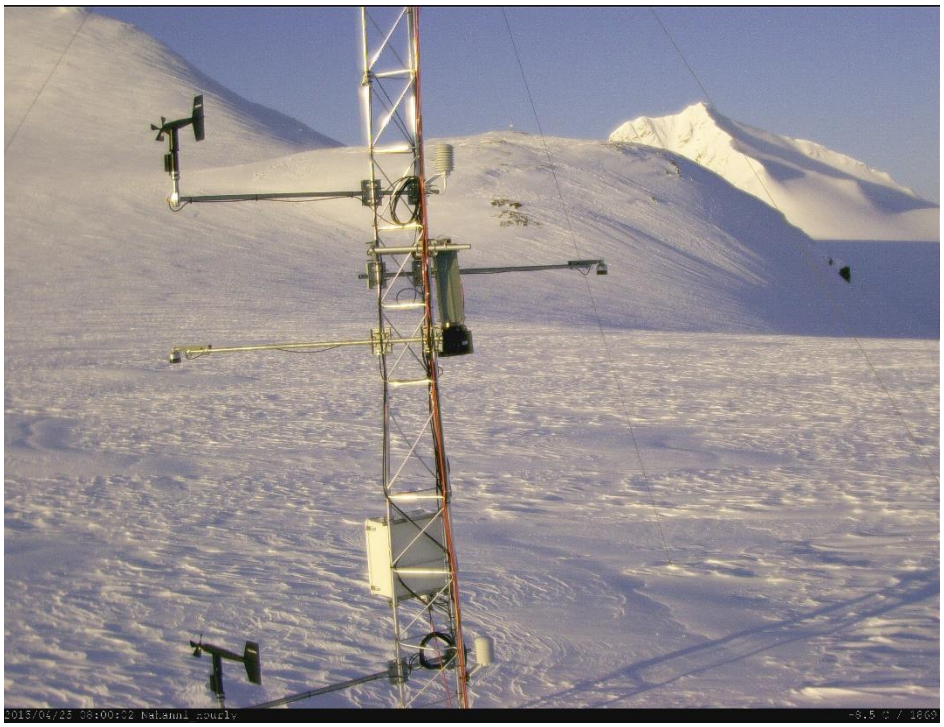

Figure 7: Typical snow surface after scour, April 25th, 2015

5.1.3 Wind

Wind speed results indicated an expected regime for winter in which the average wind speed of the upper sensors was largest (Table 4 and 5), which was the case in all months except one month in S1 (November), when the 140 cm speed range exceeded that of the 430 cm sensor. Measurements of zero are eliminated, as these are likely due to rimmed sensors and this could occur during any actual wind speeds. Overall, S1 showed more month-to-month variability than S2, for which means were relatively consistent throughout the season.

Table 4. Wind speeds in m/s by sensor and month for 2014-2015. S1 monthly averages and top sensor monthly maxima.

	Sept	Oct	Nov	Dec	Jan	Feb	Mar	Apr
915 cm maximum	6.0	7.2	4.6	5.4	7.0	6.0	6.4	6.8
915 cm average	3.3	4.3	2.9	2.8	3.9	3.5	3.5	4.0
430 cm average	3.2	4.2	2.2	2.7	3.8	3.3	3.4	3.8
140 cm average	3.0	3.8	2.5	2.4	3.4	3.0	3.0	3.2

Table 5. Wind speeds in m/s by sensor and month for 2015-2016. S2 monthly averages and top sensor monthly maxima.

	Sept	Oct	Nov	Dec	Jan	Feb	Mar	Apr
915 cm maximum	6.7	6.0	7.2	5.7	6.5	6.0	5.5	6.7
915 cm average	3.6	3.3	3.9	3.2	3.5	3.6	3.1	4.0
430 cm average	3.4	3.2	3.7	3.1	3.5	3.4	3.1	3.8
140 cm average	3.2	3.0	3.4	2.9	3.0	2.9	2.6	2.9

During S1, wind direction for the lowest sensor was unusable due to an error during deployment. The direction of the top sensor changed by approximately 20 degrees on approximately January 20th, a problem that was correctable. This was identified from plotting the differences in wind directions of the various sensors while studying wind profile. There were no issues with wind speed for either sensor due to these problems. There were no issues with comparisons of wind direction between the two seasons because they are done with the mid height sensor.

Katabatic winds were observed whereby the wind directions were oriented down-glacier (southeast) and the wind speed was fastest for the lowest sensor and slowest for the highest sensor, with the middle sensor being in between. These values were sustained for extended periods of time as evidenced by their manifestation in the hourly average

data. Of the 672 to 744 hours of measurement per month, most months had between 100 and 200 instances of the reversed profile. Typical speeds were 1, 1.5, and 2 meters per second for the 940, 430 and 140 cm sensors, respectively. There was no pattern due to seasonality or diurnal variation that could be determined. A wind direction approximately 160 degrees, approximately down-glacier, predominated. Munro (2006) observes that studies on Peyto glacier in the Canadian Rocky Mountains suggest a maximum glacier wind speed at a height above the ice on the order of 5 meters or more, consistent with studies on other glaciers. For the Bologna glacier, the decrease in wind speeds between the lowest sensor at 140 cm and the middle sensor at 430 cm would suggest a maximum speed closer to the glacier surface.

Overall, differences in direction between the high and mid sensor are predominantly between +/-5 degrees for most wind speeds, although differences of up to 20 degrees are observed for wind speeds below 2 m/s. The top anemometer was observed on a few occasions to have an opposite wind direction from the mid sensor. This is perhaps indicative of a very shallow katabatic flow, with the top sensor being outside of its influence.

The general pattern of wind direction from the mid sensor indicated a tendency to favor the southeast direction, which is the down-glacier direction. (Figures 8 and 9). In certain months, west, southwest, or northwest directions were frequent. These all align with topographical low points in the vicinity of the weather station.

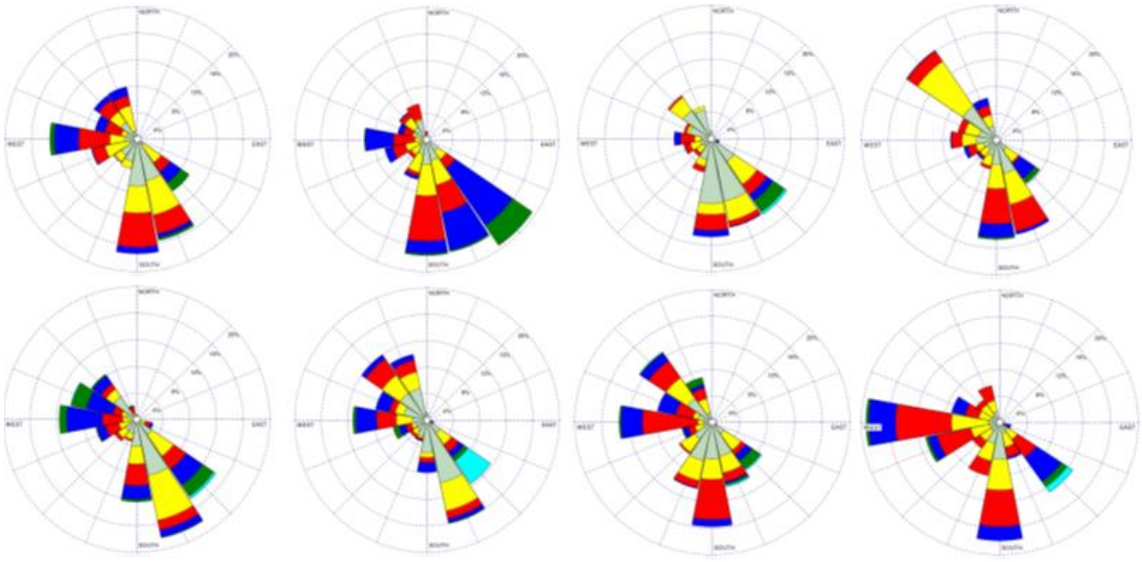

Figure 8. Wind Roses for S1. Top Row, left to right: September to December. Bottom row, left to right: January to April. The colors correspond to, from innermost to outermost, in m/s: grey, 0.5-2, yellow, 2-3.5; red, 3.5-5.5; blue, 5.5-8.5; green, 8.5-10.5; light blue, 11 +.

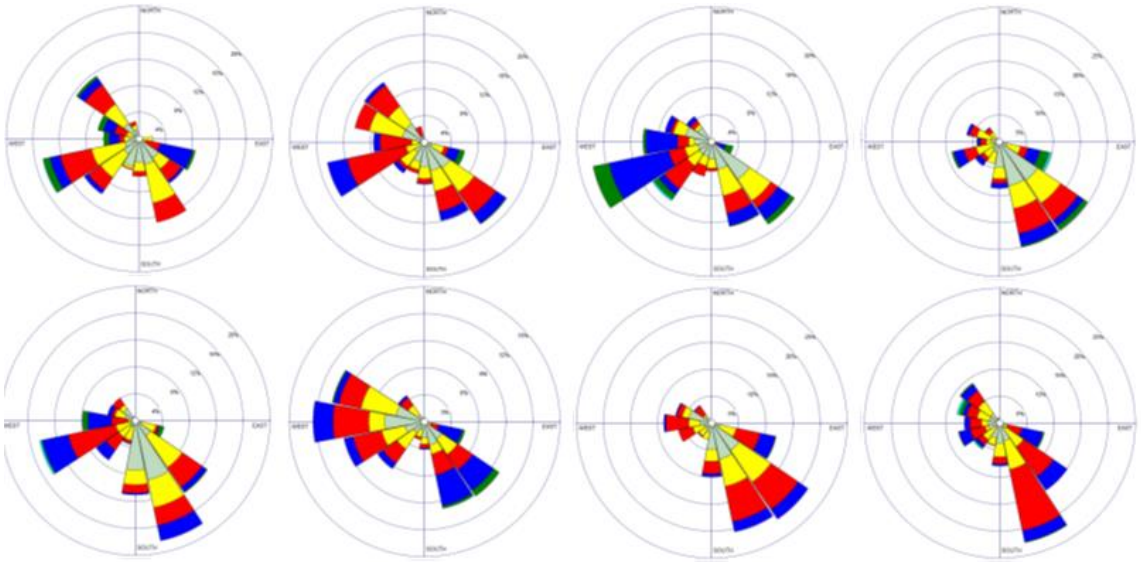

Figure 9. Wind Roses for S2. Top Row, left to right: September to December. Bottom row, left to right: January to April. The colors correspond to, from innermost to outermost, in m/s: grey, 0.5-2, yellow, 2-3.5; red, 3.5-5.5; blue, 5.5-8.5; green, 8.5-10.5; light blue, 11 +.

5.2 Snowfall event determination

The raw snow depths, 3-hour running average, and algorithm-triggered events are plotted for S1 and S2 in Figures 10 and 11, respectively. Only events that are larger than 5 cm, lasting longer than 3 hours, and verified to be snowfalls and not redistributions are shown. Individual accumulations separated by 12 hours or less were classified as sub-events part of one larger event if synoptic conditions allowed. All accumulations, including those less than 5cm, were added to event totals if they occurred between the start of the first sub-event and end of the final sub-event. Justification on these thresholds and other distinctions in STA output are included in the discussion, as the methodological design of the STA is a product of this study.

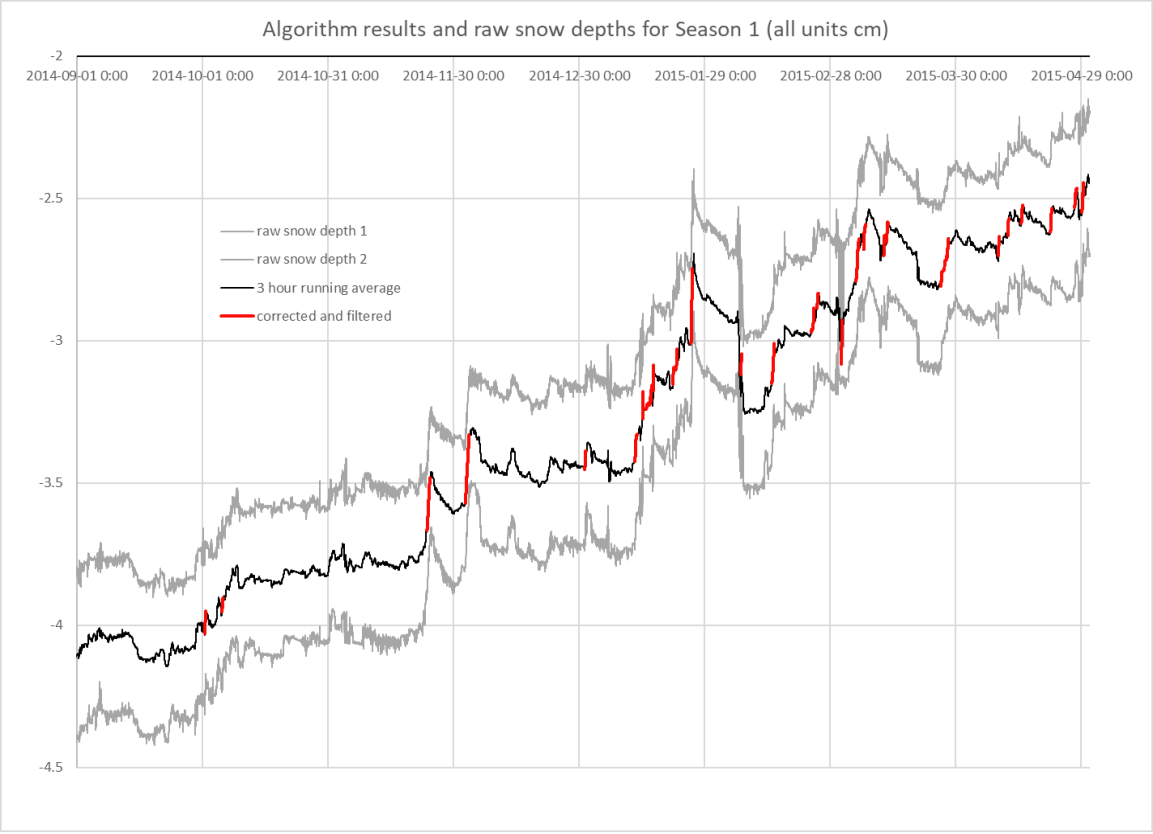

Figure 10. Algorithm-detected snowfall intervals, 3-hour running average, and raw snow depths for S1

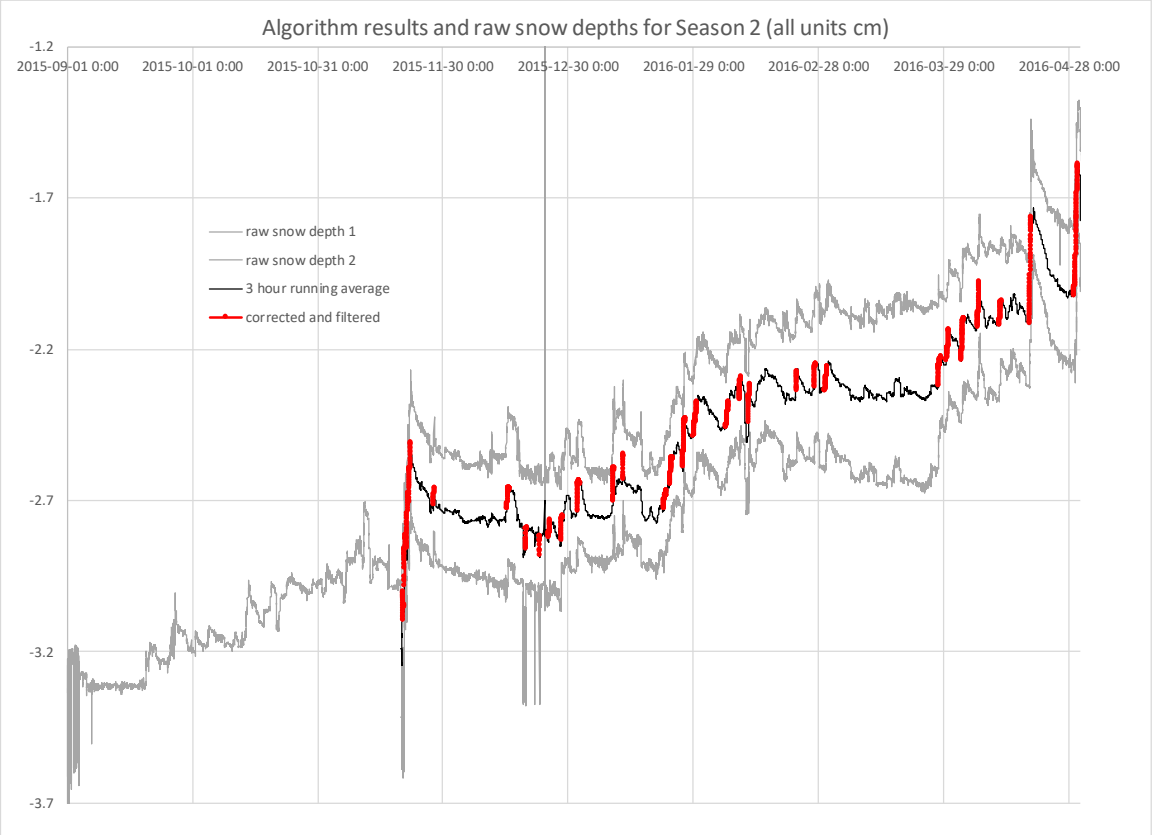

Figure 11. Algorithm-detected snowfall intervals, 3-hour running average, and raw snow depths for S2

The event metadata for large events is tabulated in Table 6. Times are adjusted to UTC from MST to facilitate comparison to reanalysis plots. The total is calculated from the beginning of the first sub-event to the end of the last sub-event (for events without sub-events, it is simply from the beginning to the end).

Table 6. Large snowfall event metadata

Event ID	Start month day time	End month/day/time	Total (cm)	Sum of algorithm events (cm)
S1E1	11/23/1300	11/24/2200	25	26
S1E2	12/03/0500	12/04/0800	26	26
Pre-S1E3	1/12/1600	1/26/0300	48	55
S1E3	1/26/0300	1/26/1800	28	26
S1E4	03/04/1500	03/09/1300	37	56
S2E1	11/20/1100	11/22/1300	71*	63*
S2E2	01/20/1800	01/30/1300	41	44
S2E3	03/28/0300	04/07/0500	36	50
S2E4	04/19/0000	04/19/1100	41	40
S2E5	04/30/0100	04/30/1300	42	42

* start of this event unclear due to erroneous readings from one SR50A sensor.

In table 7, various statistics for snowfall in both seasons are presented. The snowpack depth signifies the total depth at the end of the season, as described in section 5.1.1 above, and is included for comparison. The STA total >5cm and STA total <5 cm show the proportion of algorithm detected events over and under that threshold and the sum is the STA total. All three are presented to compare between the two seasons. The events total is the sum for each respective season from Table 6 on large snowfall event metadata from the sum of algorithm events column. The column of S1/S2 highlights the difference between S1 and S2 for each parameter. Figure 12 gives a comparison by month of algorithm-triggered events to demonstrate monthly variability. For S2, the period from the beginning of September until November 20th is not considered. The algorithm can not be applied due an issue with the sensor as previously discussed, however it is apparent that at least two events 10-20 cm would have been detected in each of September, October, and November. Based on these numbers, there do not appear to be any major events, however without the second snow depth sensor it cannot be confirmed. September in S1 has no STA-detected events, and while October sees a significant total accumulation, the algorithm is infrequently triggered.

Table 7: STA totals for S1 and S2

	S1	S2	S1/S2
Snowpack depth	165 cm	178 cm	93%
STA total	525 cm	640 cm	82%
STA total < 5 cm	281 cm	211 cm	133%
STA total > 5 cm	244 cm	429 cm	57%
Events total	134 cm	239 cm	56%
Event total / STA total > 5 cm	55%	56%	N/A
Event total / STA total	26%	37%	N/A

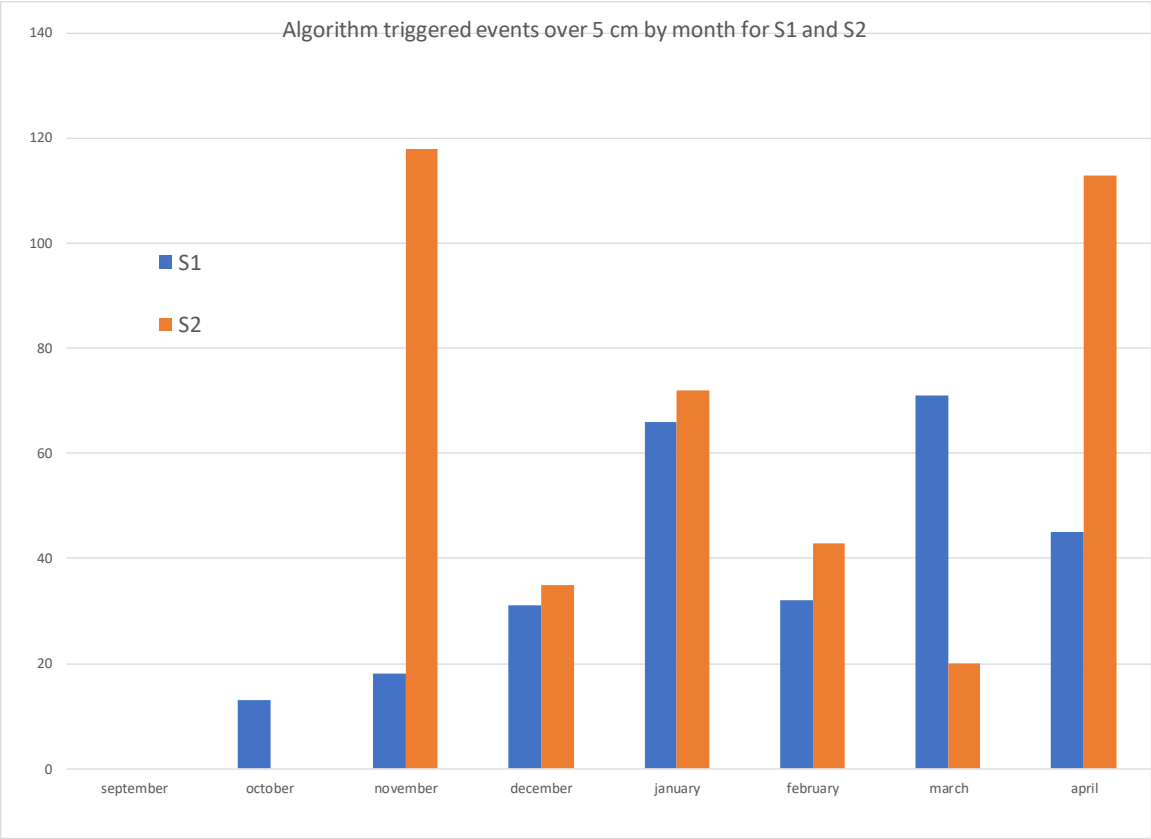

Figure 12. Sum of the snowfall totals of all STA-triggered events over 5 cm by month for S1 and S2

5.3 Large Snowfall Event Narratives

The analysis of synoptic conditions present during large snowfall events are described with select AWS data, reanalysis plots and back-trajectories. Plots in figures are labelled A, B, C etc from left to right and up to down.

5.3.1 S1E1, S1E2

Events S1E1 and S1E2 occur within one week of each other at the start of S1, and exhibit approximately the same amount and rate of snowfall. A strong stationary low-pressure system centered off the west coast of Alaska is present for the entirety of both events (Figure 13A and 13B). Both events coincide with a ridge at 500mb in place over the western United States coast during the event (Figure 13C and 13D); during S1E2 the ridge stalls for some time, however during S1E1 it moves rapidly.

Before the S1E1 event, the Hysplit trajectories show advection of high moisture content air from off the coast of central British Columbia. This is supported by what appears to be some northward movement of the large maritime air mass into central BC, however, the precipitable water over the study area remain very low throughout, approximately 2-6 kg/m^2 (Figure 14). The 500 mb geopotential heights and surface low-pressure also support this. The winds at 750 mb near the station veer over time, from due south 24 hours before the event to due west during the event. The start of the event corresponds exactly to when the wind direction at the study site switches from approximately 150 degrees to 300 degrees, and the end of the event occurs very close to the switch back from 300 to 150. Winds aloft are considerably faster during the event than before or after, and the same is true of winds at the weather station. By contrast, the S1E2 event occurs with a visible plume of moisture impacting the northern BC coast and moving due east directly over the study area. The same moisture content of 2-6 kg/m^2 during S1E1 is observed before and after S1E2 but during the event this value rises to 6-10 kg/m^2 (Figure 15). The low-pressure system is situated slightly more to the north during this event and moves over inland Alaska. For both S1E1 and S1E2, Hysplit trajectories transit from ocean to over land near the Copper River in southern Alaska (Figure 16) and rise to a high elevation. Low altitude trajectories over the BBI do not have realistic trajectories. Wind speeds at the weather station do not show much variation

before, during, or after the event, and the direction stays fairly constant from the west as well.

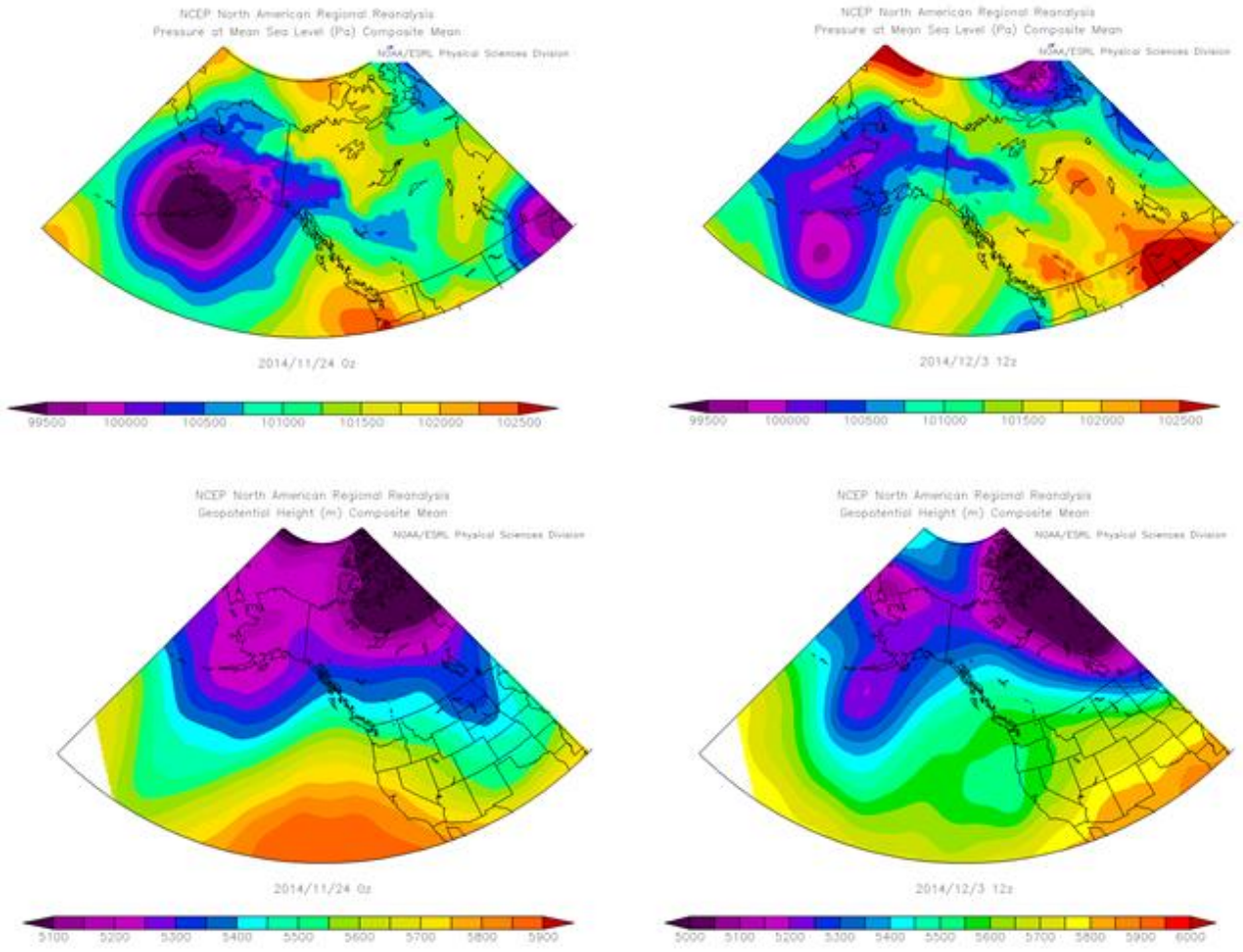

Figure 13: A) S1E1 Mean sea level pressure 11/24/0000z; B) S1E2 Mean sea level pressure 12/03/1200z; C) S1E1 500 mb geopotential height 11/24/0000z; and D) S1E2 500 mb geopotential height 12/03/1200z.

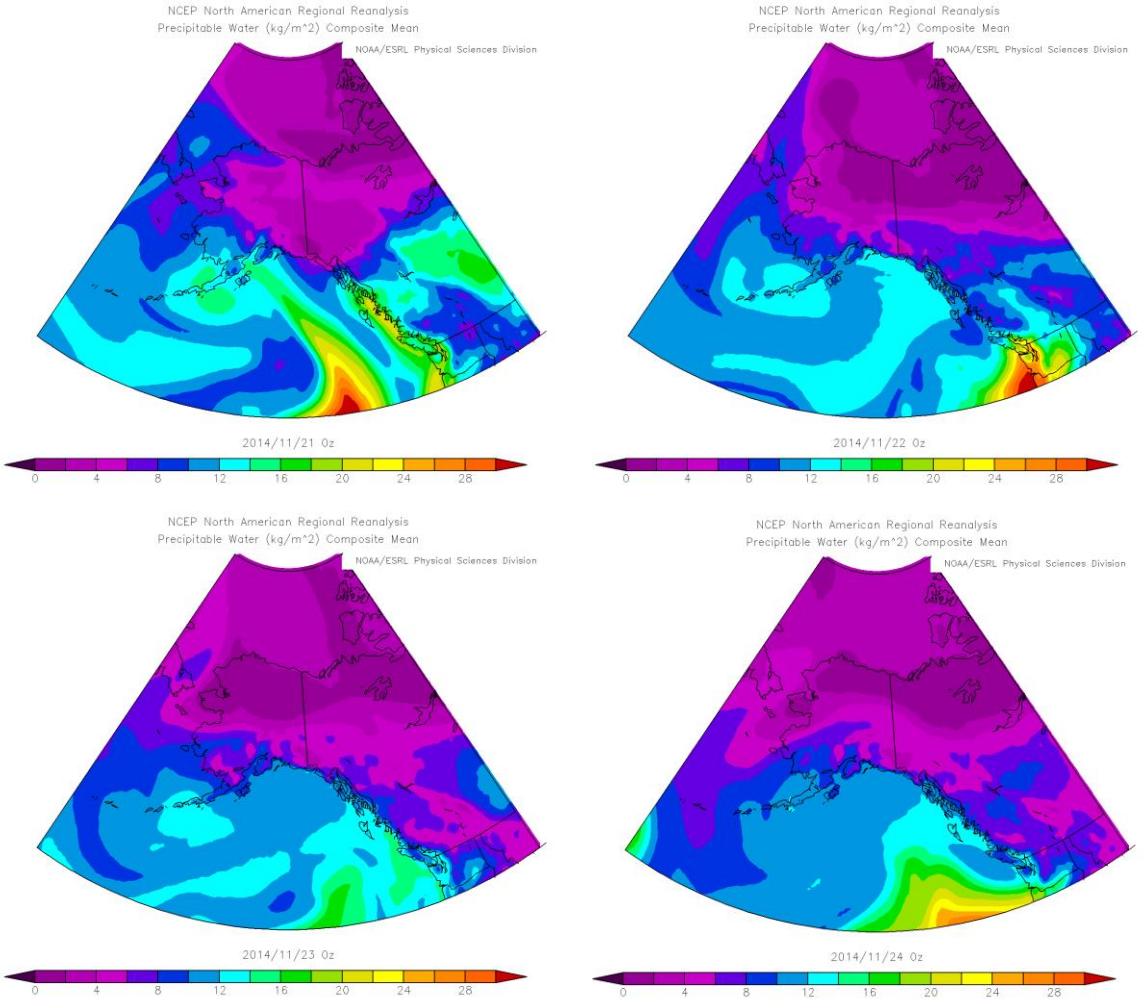

Figure 14: Precipitable water (kg/m2) for S1E1 at A) 11/21/0000z, B) 11/22/0000z, C) 11/23/0000z, D) 11/24/0000z

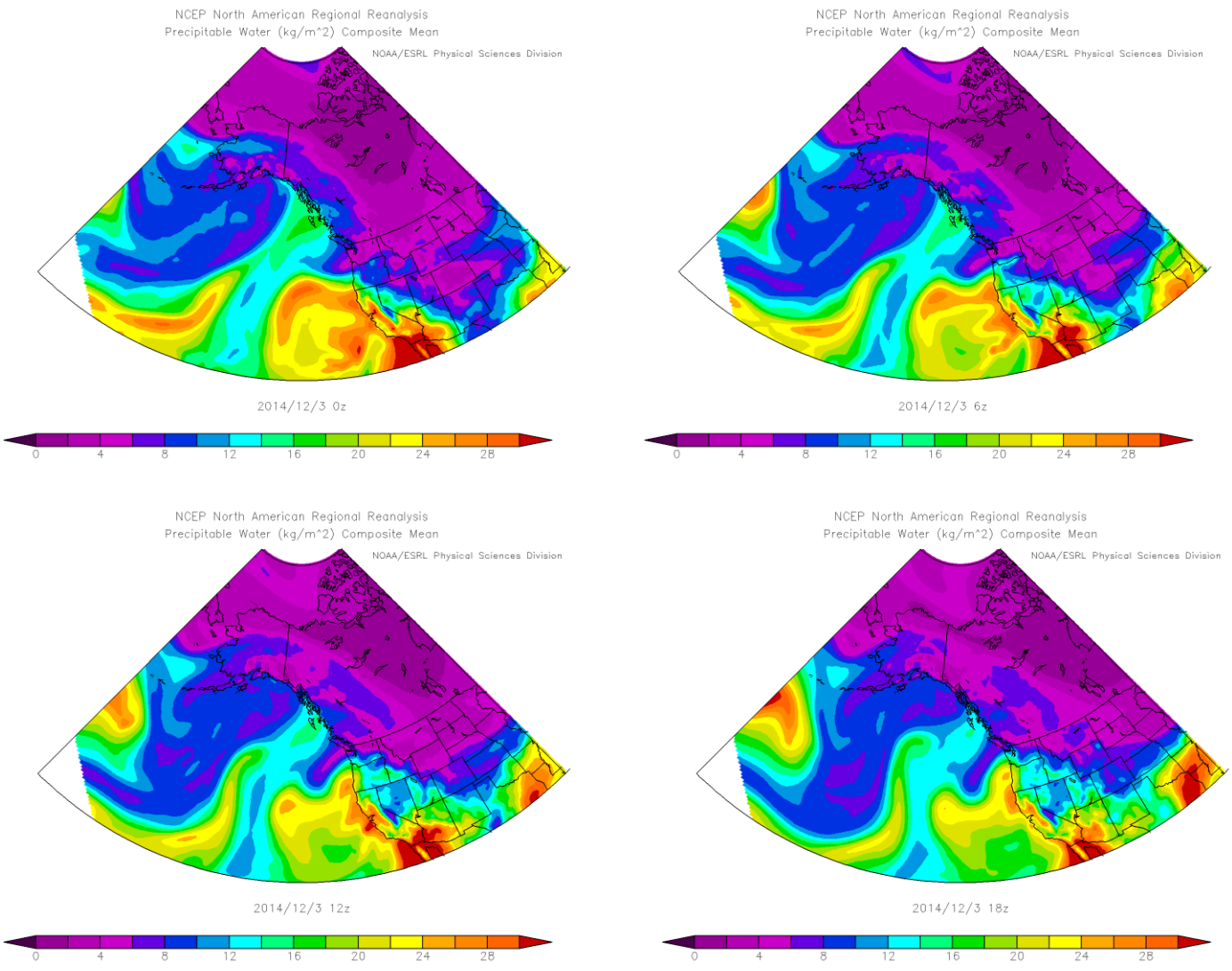

Figure 15: Precipitable water (kg/m2) for S1E2 at A) 12/03/0000z, B) 12/03/0600z, C) 12/03/1200z, D) 12/03/1800z

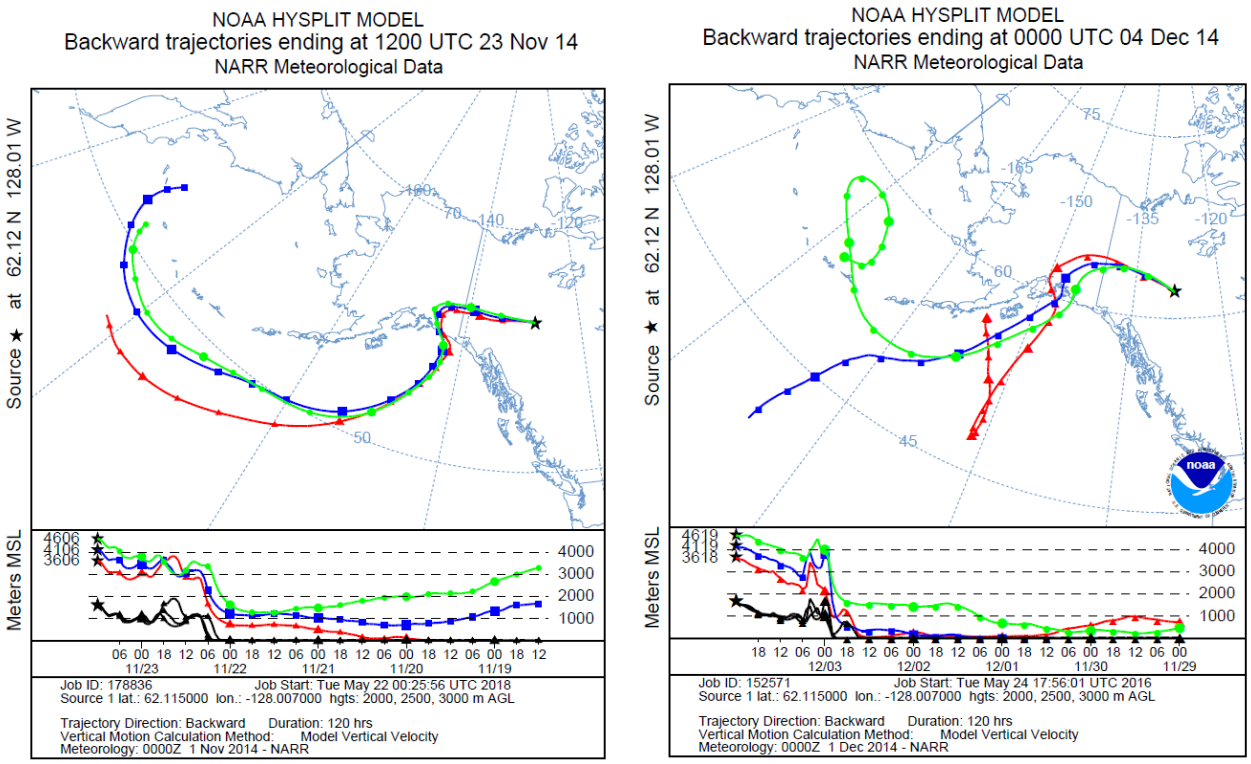

Figure 16: Hysplit trajectoies for A) S1E1 11/23/1200Z B) S1E2 12/04/0000Z

5.3.2 S1E3, S2E2

S1E3 is the only large event qualified for analysis from a series of short but high rate snowfalls from January 12th to 26th, or Pre-S1E3. S1E3 is the culmination of this series of events (Figure 17). While the snowfalls prior to it cannot be considered as sub-events due to discontinuities in the synoptic mechanisms responsible, it is illuminating to consider the conditions present prior to S1E3 and they are therefore described briefly. During pre-S1E3, two consecutive strong low-pressure systems (center < 97 kPa) move into the Gulf of Alaska and dissipate. S1E3 does not begin until the second low-pressure system is gone. Large moisture plumes successively impact the British Columbia Coast pre-S1E3, with concentrations up to 15 kg/m^2 resolved over the BBI (not shown), however the last of these appears to have exited the area during the S1E3 event. Winds at the AWS do not change significantly immediately before, during, or after the event and neither do the Hysplit trajectories insofar as the location as their transit over land.

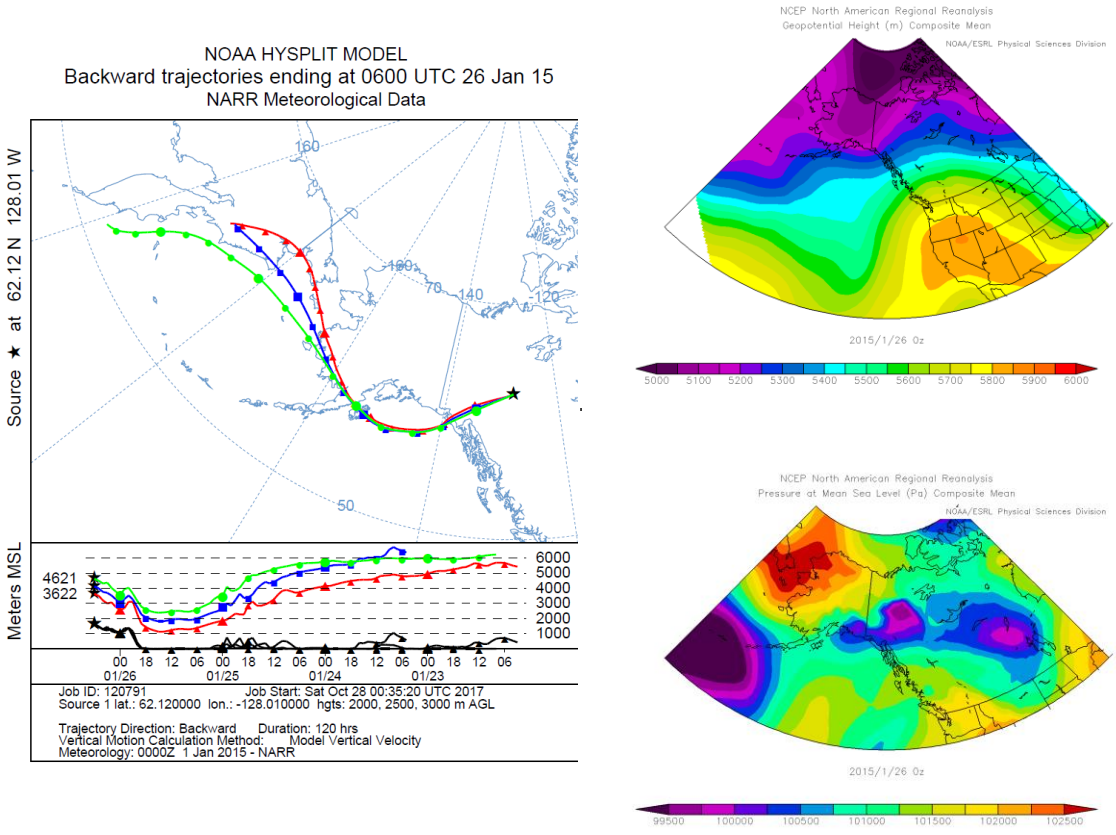

Figure 17: S1E3 01/26/0600Z A) Hysplit trajectory; B) Geopotential height; C) Mean sea level pressure.

S2E2 is similar to S1E3 and pre-S1E3 in duration and total snowfall. It also features two strong low-pressure systems (center < 96.5 kPa) and successive moisture plumes. However unlike S1E3 it exhibits primarily sustained, slow accumulation and as such it is analysed as one event. It begins with a mature low moving into the Gulf of Alaska and dissipating, and is followed by a second low that stays in the Gulf of Alaska south of the Aleutians Islands. Trajectories show variability in location of landfall, from mainland Alaska to the BC coast (Figure 18). Wind direction at the AWS consistently shows a westerly component except during breaks in snowfall, when it switches to easterly.

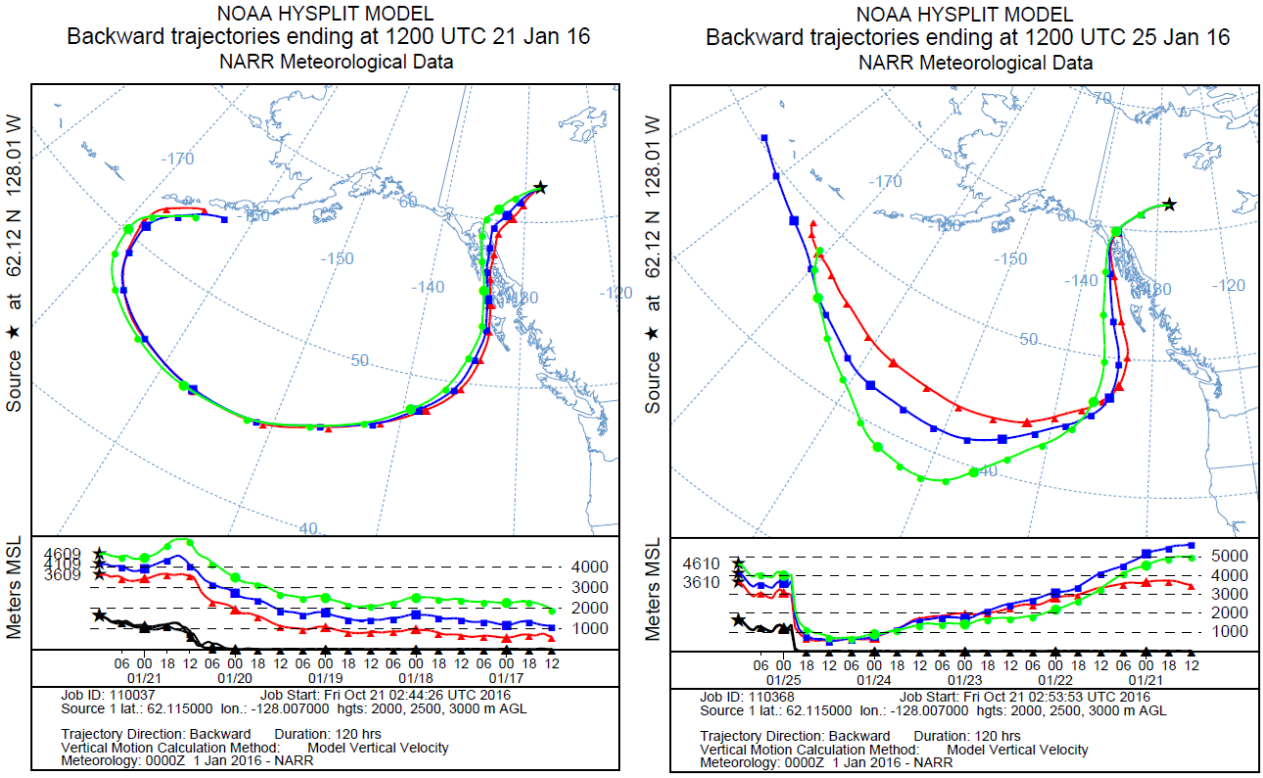

Figure 18: Hysplit trajectories S2E2 A) 01/21/1200Z B) 01/25/1200Z

5.3.3 S1E4

This event exhibits similar characteristics to pre-S1E3, with brief high accumulation rate events separated by breaks, however these are short enough that it can be considered as one event with multiple sub-events. This event does not have a distinct surface low-pressure system in the Gulf of Alaska, however two low-pressure systems move east across northern Alaska. The main break in this event occurs during the dissipation of the

first low that has moved across Alaska and before the succeeding one moves towards western Alaska. During this time, a cut-off low is formed and identifiable at the surface and 500mb level. Geopotential heights at 500 mb show a consistently zonal pattern otherwise, and winds at the weather station are approximately constant at 300 degrees for the duration of the event. Wind direction at the weather station changes from SE to WNW at the start of the event and reverses at the end. The windspeed before and after the event are slower. There are a few occurrences of winds from the SE during the event and they occur with low wind speeds. Higher wind speeds occur when the winds come briefly from the NNW. At the beginning of this event, the three higher altitude Hysplit trajectories show consistency vertically and horizontally. The opposite is true for the low elevations. Later on in the event, the higher and lower sets of trajectories show cohesive motion (Figure 19).

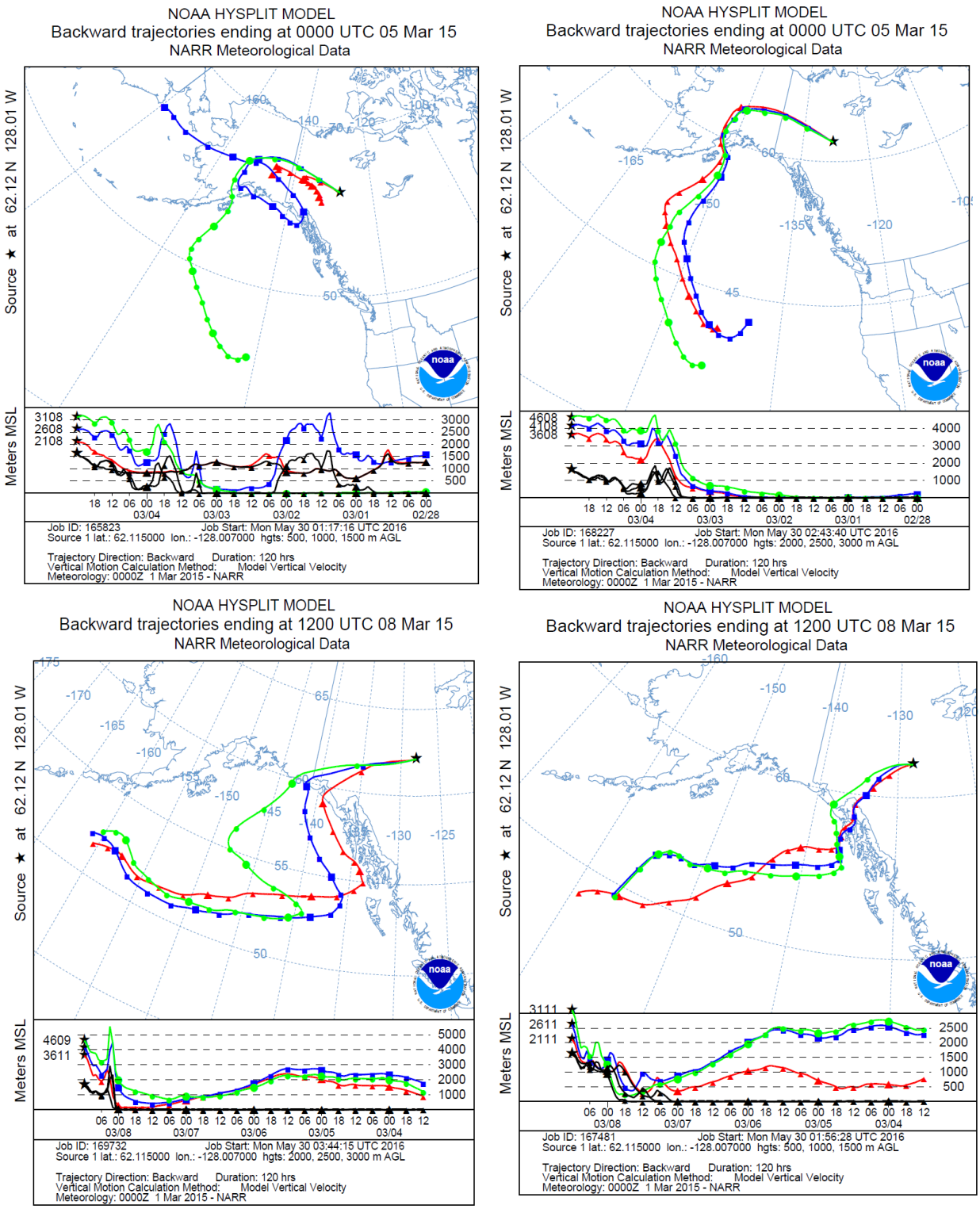

Figure 19. Hysplit trajectories S1E4 A) Low ending elevations 03/05/0000Z; B) High ending elevations 03/05/0000Z; C) Low ending elevations 03/08/1200Z; D) High ending elevations 03/08/1200Z

5.3.4 S2E1

The first event of the second season is the largest observed during the two seasons. This event consists of four sub-events that result in a total of 70 cm of snow in just over 2 days. Prior to the beginning of the first event, a large low-pressure system approaches the Alaska coast from the west (Figure 20A). A cold, dry airmass covers most of Canada and two large southwesterly extending moist airmasses stretch across the Central and North Pacific (Figure 20C).

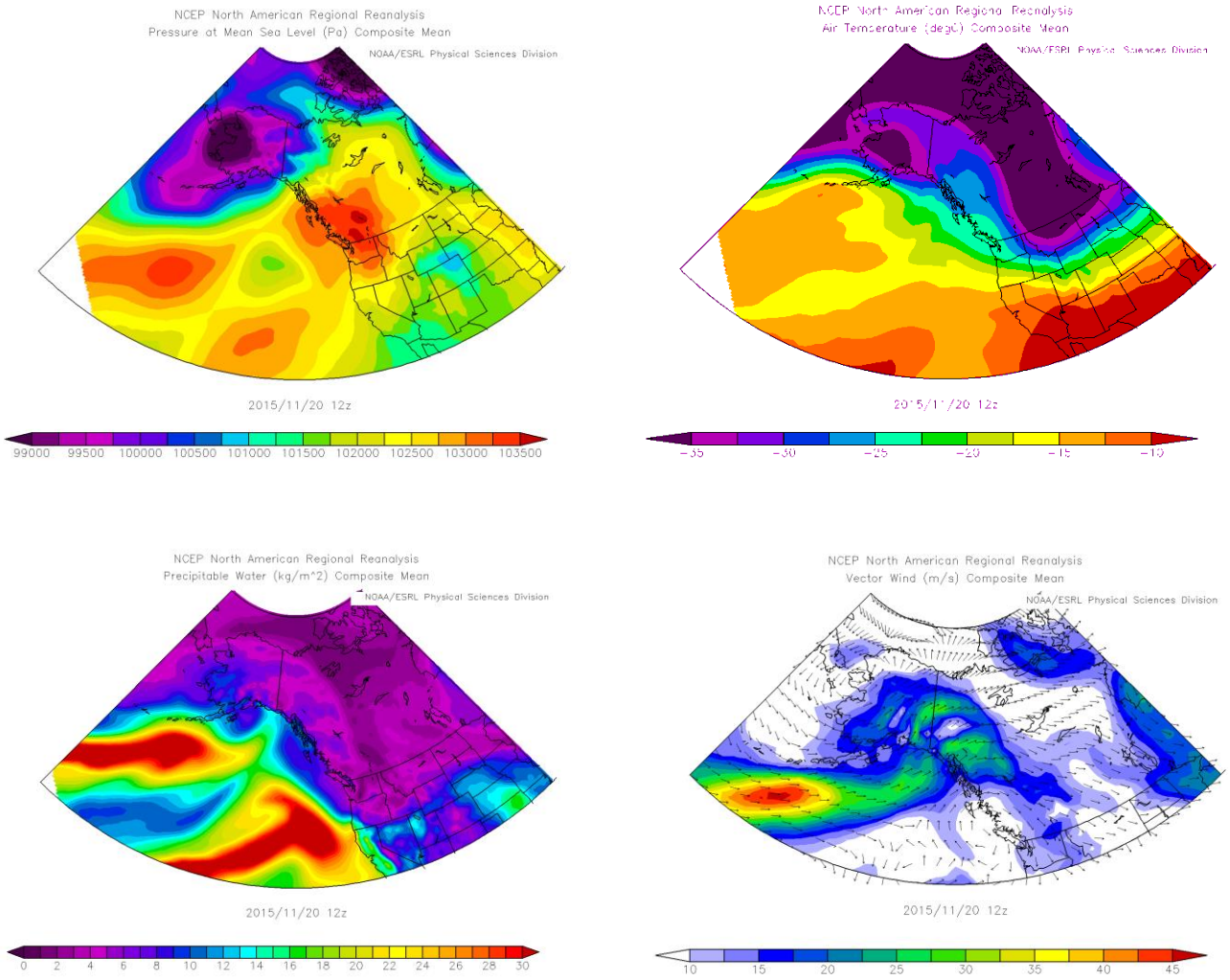

Figure 20: S2E1 11/20/1200Z A) Mean sea level pressure; B) Air Temperature 500 mb; C) Columnar precipitable moisture; D) Vector wind 750 mb

Immediately prior to the first subevent, a strong low-pressure system is over Alaska and a weak high-pressure system is over B.C. The temperature at 500mb (Figure 20B) and wind at 250 mb show that a ridge in the jet stream is present over the Yukon. Advection of the more northerly of two moisture concentrations is occurring. At 1100Z on November 20th, sub-event 1 snowfall begins, wind direction at the station switches from SE to WSW, and wind speeds increase (Figure 21). Temperature at the study site rises rapidly from ~ -30 to -15 °C. Despite the wind direction shifts at the station, Hysplit trajectories before and during the first subevent are constant from the west immediately prior to moving over the icefield. Prior to the event, they are high altitude and do not come from the moist maritime air mass. After the beginning of the event, they show an approach from the Alsek River valley. Winds at 750mb (Figure 20D) support this, and appear to be approximately twice as fast over the icefield on 11/20/12z vs 11/20/0z. A lobe of moisture with north-south orientation is observed to move over the coast ahead of the main moist air mass. The event ends as this lobe passes, without a significant change in Hysplit trajectories or AWS winds.

By the start of the second sub-event (21/00), the low-pressure centre over Alaska has deepened and the main moisture plume is impacting the coast. Reanalysis plots suggest that more moisture is moving inland than during the first sub-event, however the timing of arrival of this moisture does not appear consistent with the timing of snowfall at the AWS. The event ends with wind speeds dropping dramatically both at the 750mb level and AWS, and the wind direction changes to the SE. Within the second break, a small increase in wind speed corresponds exactly to a reduction in snow depth.

The third subevent begins with snowfall resuming at 21/17:30 along with an increase in wind speed and a return to WSW wind direction at the AWS. The low-pressure system, which has been moving east continuously, moves over the study area. The ridge in the Jetstream reduces in amplitude and flow becomes more zonal. Hysplit trajectories are situated at low altitude over the ocean right up until they meet the coast (Figure 22).

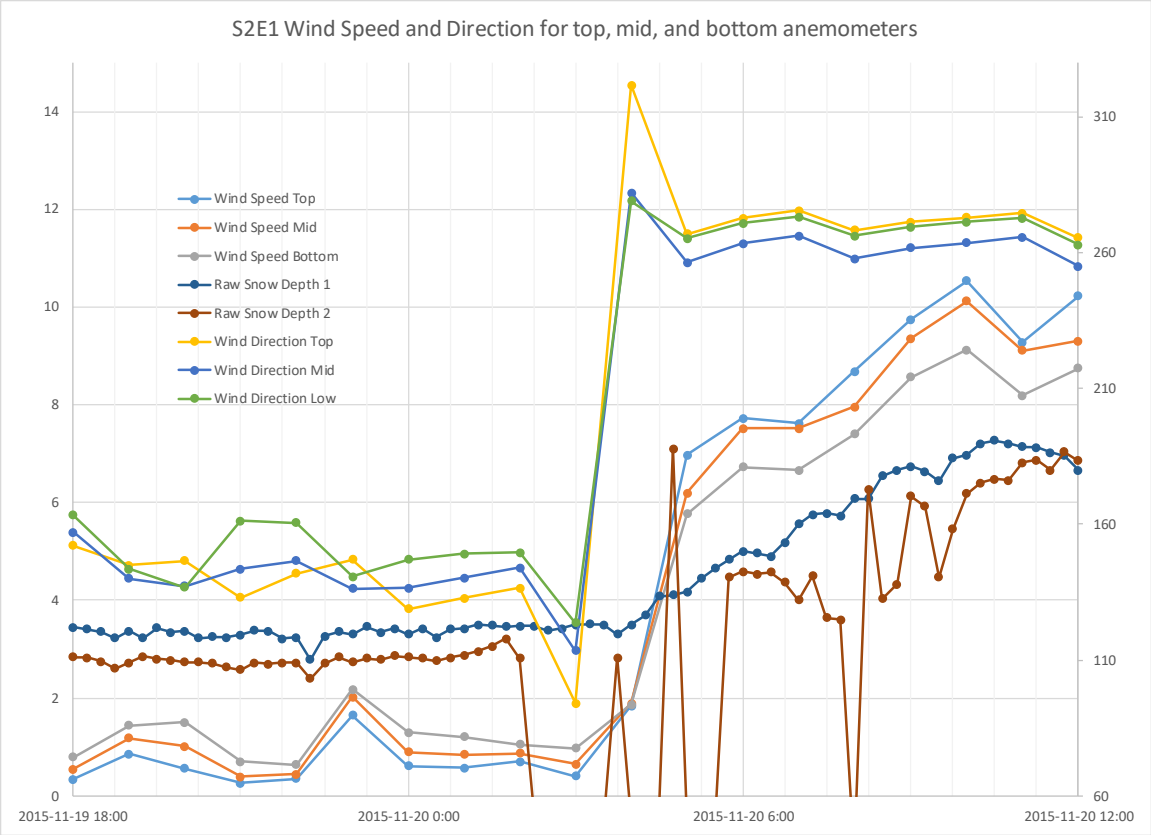

Figure 21: Hourly average wind speeds (m/s, left y-axis) and directions (degrees, right y-axis) and fifteen-minute raw snow depths (scaled values for reference)

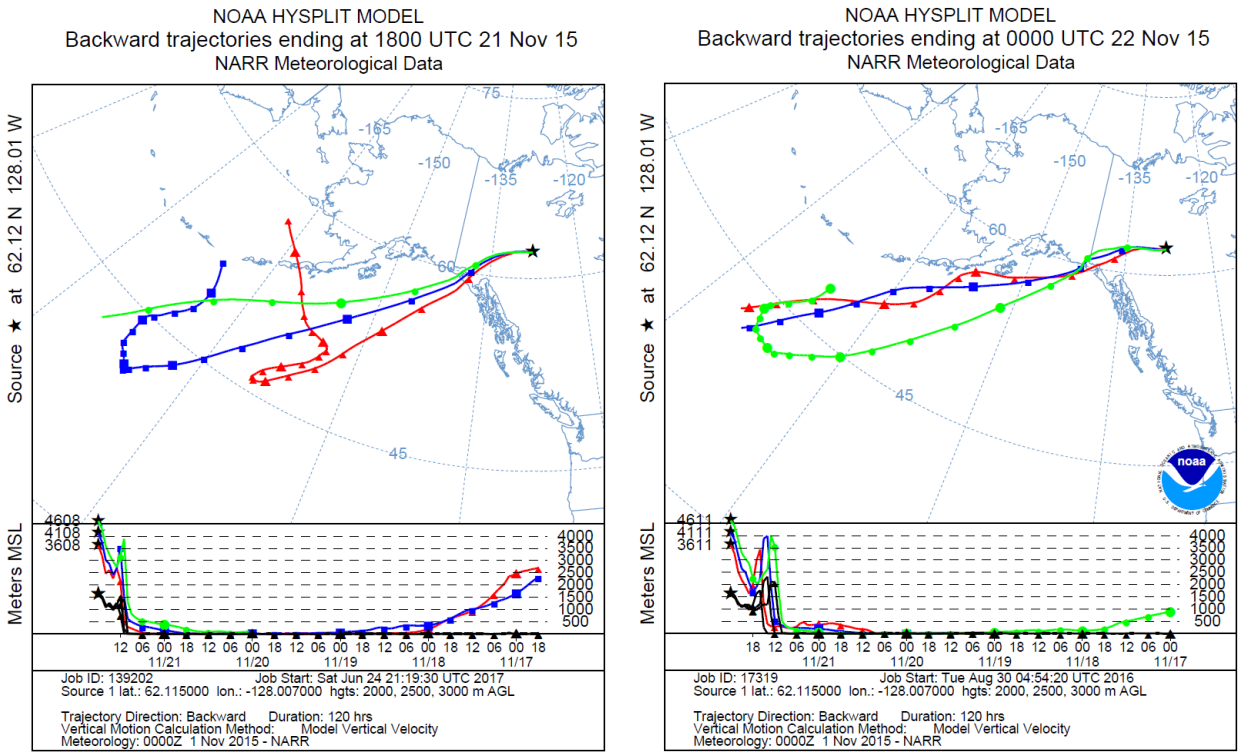

Figure 22: Hysplit trajectories A) 11/21/1800Z B) 11/22/0000Z

The third subevent ends and the third break occurs without any noticeable changes in synoptic conditions. The beginning of the fourth event coincides with a peak temperature of around -6 °C. Throughout, the main concentration of moisture passes from NNW to SSE to the south and on the periphery of the study area. The reanalysis plots of accumulated precipitation and of precipitation rate suggest that heavy snowfall occurred to the west of the icefield. The wind directions at the study site remain between 250 and 300 degrees, which persist well after the fourth subevent. Winds at 500 mb are weak and shift to southerly during the event.

5.3.5 S2E3

This event occurs when a large trough over Alaska and a large ridge over the coast funnel a large moisture plume NE towards the study area. The up-glacier wind direction during snowfall is more northerly than most other events: between 250 and 350 degrees. The surface and 500 mb pressure levels show a synchronous evolution through the event; at 500 mb the ridge is seen to move over the coast and amplify (Figure 23). A low-

pressure system is present throughout most of the event in the vicinity of the Aleutian islands.

After initial contact with the coast, which corresponds to the start of the first subevent, the main moisture plume ceases eastward movement and begins to move northwest, changing its orientation from SW-NE to NNW-SSE, and a lobe of moisture separated from the main plume continues to move overland. The second subevent ends as the separated moist airmass moves away from the area. The main plume's westward motion stops shortly after, and resumes eastward movement. The third and fourth sub-events occur while the moisture plume passes over.

Hysplit trajectories show variability in entry point and altitude. Many hysplit trajectories do not come down to sea level, and for those that do, they occur 3 or 4 days prior to arrival at the icefield. The high trajectories are very stable and are not perturbed as they move through the Coast Mountains.

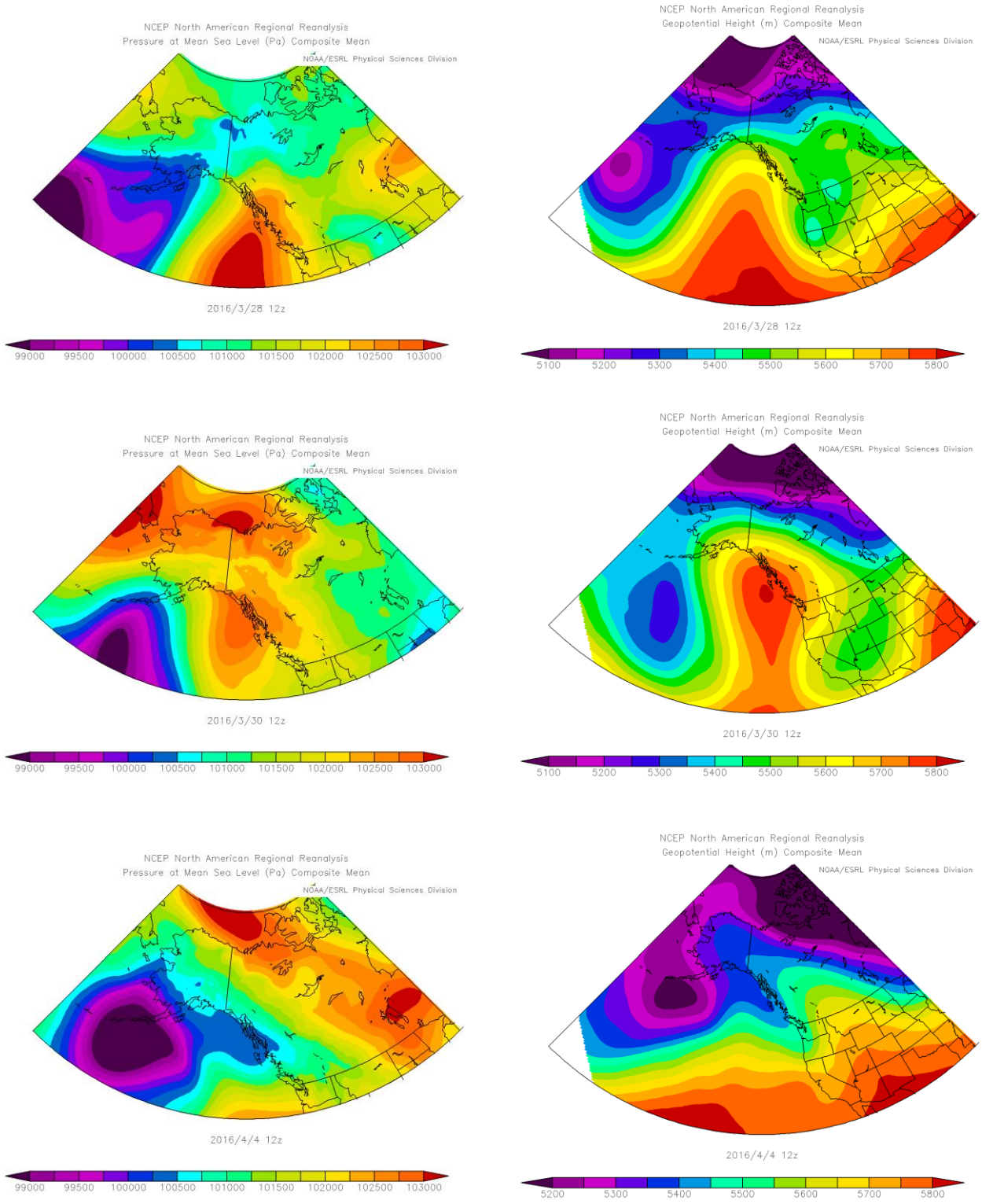

Figure 23: S2E3 A) Mean sea level pressure, 03/28/1200Z; B) Geopotential height 500mb, 03/28/1200Z; C) Mean sea level pressure, 03/30/1200Z; D) Geopotential height 500 mb, 03/30/1200Z; E) Mean sea level pressure, 04/04/1200Z; F) Geopotential height 500 mb, 04/04/1200Z

5.3.6 S2E4, S2E5

Two events in late April of S2 had the highest snowfall rates of any of the events considered in the two seasons. S2E4 and S2E5 deposited over 40 cm each in 11 and 8 hours, respectively. Both events occurred when a low-pressure system stalled over the Aleutian Islands. The low was not particularly strong; rather its lack of movement was the important aspect. Hysplit trajectories show a consistent pattern throughout both events with entry over the central coast of British Columbia and remain at very low altitudes (<hundreds of meters) as they move towards the study area (Figure 24). Winds at the study area for both events show that timing of wind direction change was closely linked to the start of snowfall. The end of the events occurred when the moisture moving overland has passed the icefield and continues on a northerly trajectory.

S2E4 shows average wind speeds of up to 14 m/s at the study site during this event. The speed and direction is maintained for a short time after the end of snowfall, then speed drops dramatically, to below 1 m/s on 04/20/0000, 24 hours after the start of the event. Wind direction at the study site switched to ~150° at this time, and winds aloft are northerly.

In the day prior to S2E5, wind direction moves clockwise as wind speed decreases until 04/29/1500 MST, when all three anemometers recorded directions between 100° and 110°. One hour later, the lowest wind speed of the event is recorded, less than 1 m/s, and the wind direction changes back to an average of 300°-310°, and snowfall begins. After the event, wind direction and speed at the station remains constant.

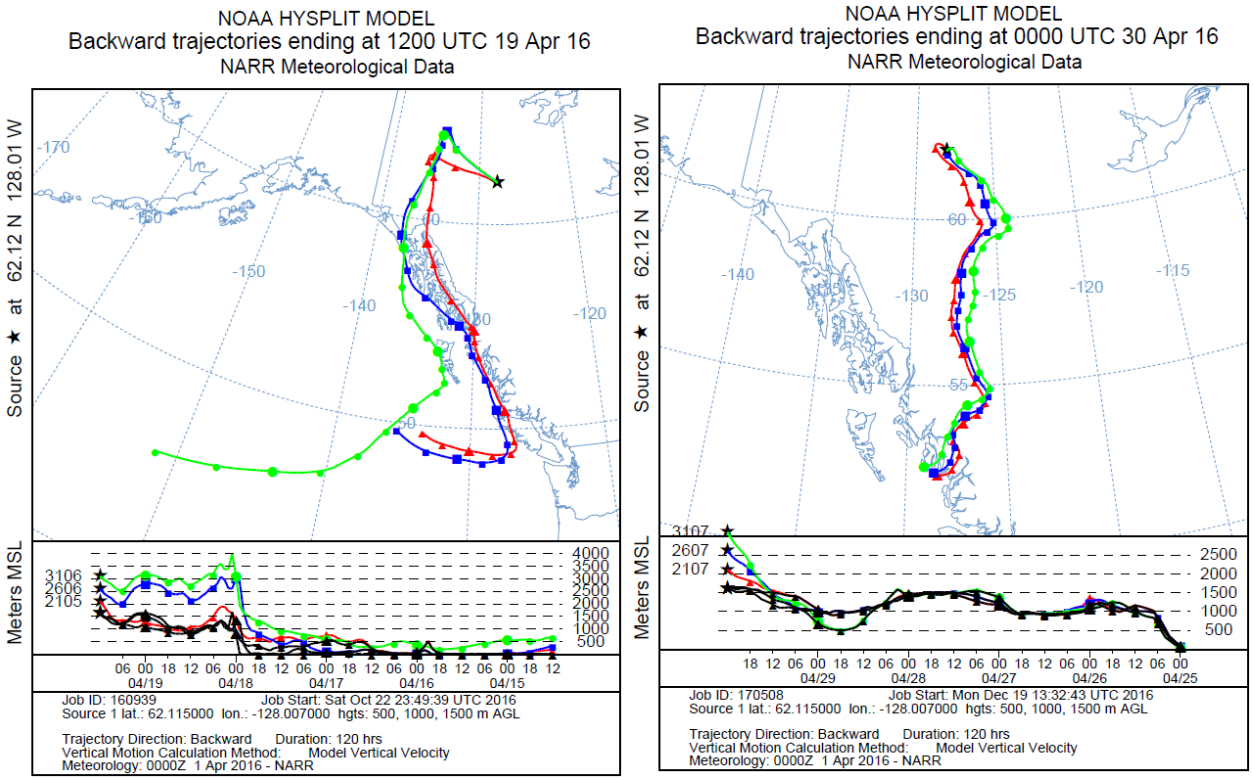

Figure 24: Hysplit A) S2E4 04/19/1200Z B) S2E5 04/30/0000Z

6. Discussion

The analysis of the largest snowfall events at the BBI was the primary purpose of this study, and it was investigated using AWS data, meteorological reanalysis plots, and trajectory modelling. This is the archetype research methodology for investigating the origin and pathway of moisture leading to precipitation over a study region. For this study, the modification to this scheme is the intra-event analysis. This is in contrast to most studies, in which events are analysed on much larger spatial and temporal scales, generally utilizing data from multiple stations over a large area for multiple seasons. Events are characterized on a coarser scale such as days of consecutive increase of SWE (Serreze et al, 2001) or maximum 1-day accumulations (Alexander et al, 2015). These metrics allow regional comparisons and determination of frequency of various synoptic types or moisture pathways, however they cannot be used to elucidate the mechanisms or variations occurring within individual precipitation events.

The STA was developed to precisely quantify the timing of events through high temporal resolution allowing sub-hourly analysis. This is due to the triggering mechanism of beginning and end of snow depth increase. The running average reduces such sensitivity in order to eliminate disparity between the individual acoustic sensors and the average snow depth surrounding the AWS. Variations in rate and continuity of snowfall, however, still cause interruptions in the STA which can simply be natural intermittent breaks in large snowfalls. These occurrences must therefore be identified as either separate entities or grouped appropriately, leading to classifications of single events or compound events consisting of sub-events which are separated by breaks of various duration. Most breaks shorter than 6 hours did not signify a modulation of synoptic activity, and for some breaks there was no distinguishable cause except when it was evident that the wind direction was the controlling factor. Breaks between approximately 6 and 12 hours were generally caused by modest synoptic changes, for example those that alter the entry point of moisture, or the passage of lobes of lower moisture within the air mass. Intervals longer than 12 hours without snowfall were not considered breaks, as they generally signified a shift in synoptic weather. Events separated by intervals longer than 12 hours were considered for analysis if they were individually sufficient in length, and otherwise discarded from consideration. These decisions were made on a case-by-case

basis. For example, one large moist air mass advected by distinct but sequential extratropical cyclones qualified; multiple moist air masses advected by distinct cyclones did not.

For in-depth analysis, the largest events in each season were chosen, as they provide the most substantial contribution to the total snowpack. All events over 20 cm were selected; this yielded four in the first season and five in the second season, a sufficient number for comparison of synoptic and topographical controls. STA-determined occurrences with accumulations larger than 5 cm and longer than 3 hours were evaluated individually. This threshold was selected as the minimum accumulation amount verifiable through the STA, and the 3-hour duration matches the NARR reanalysis utilized. Some accumulations larger than 5 cm occur either before or after decreases of the same magnitude. Rapid wind speeds suggest removal and subsequent deposition during a redistribution event, and in those cases the accumulations were excluded from analysis. The absence of high winds and a gradual snow depth decline suggests densification of a true snowfall and these were included.

The four major events in S1 brought a total of 134 cm and the five in S2 brought 239 cm. The total for STA > 5 cm are 244 cm for S1 and 429 cm for S2. In comparison to S2, S1 therefore has only 56% of the major event total and 57% of total STA > 5 cm. This is contrasted by the similar total season snowpack depths between the seasons: 165 cm and 178 cm, respectively. This is partly explained by the much higher contribution of total STA < 5 cm for S1 (281 cm) compared to S2 (211 cm), however the STA total for S1 (525 cm) is still considerably less than S2 (640 cm). Taken together, the aforementioned values can be understood as S1 being characterized by frequent but small average events and fewer major events and S2 exhibiting fewer but larger average events and more major events. This does not explain the apparent disparity between the similar total snowpacks between seasons and thelarger total STA count in S2. This is perhaps explained by larger snowfall events having a greater susceptibility to redistribution and ablation, or differences in snowfall density or densification rates. In both seasons, the monthly totals of accumulations larger than 5 cm in figure 12 show that large events dominate the relative totals for any individual month. Of note is that the values for S2 also do not include September and October during which malfunction by one snow depth sensor prevented STA application. During this time, the functioning snow depth sensor

appears to detect several conspicuous medium sized events that may have added up to an additional ~50 cm total. This would only increase the contrast between seasons.

It was found that commonalities existed in the synoptic conditions during most accumulations regardless of duration, total snowfall, and rate. These are represented in the composite plots that were computed from all days that include an STA > 5 cm accumulation. These are characterized by a low-pressure system centered over the Aleutian Islands and at 500 mb the geopotential height bulges north with a ridge over the coast (Figure 25). Most of the large events demonstrate these features as well. A low-pressure system at sea-level in the vicinity of the Aleutian Islands is present in all but one of the 9 events (the only exception is S1E4 with a low-pressure system over northern Alaska). The Aleutian islands are the endpoint of the North Pacific storm track; storms stall out and dissipate here. Events are shown to occur at various stages in the lifecycle of these extratropical cyclones; some as the low is still strengthening, others after the low-pressure system is no longer distinguishable. The strength of the low-pressure system therefore does not appear to be an important factor in snowfall-producing conditions. The determining factor in snowfall continuity appears to be the immobility of the low-pressure system. The four most sustained snowfall events, each with no breaks, occur with the four most stationary mslp patterns. S1E1 and S1E2 occur with near stationary and medium strength low-pressure systems. S1E3 has no visible low-pressure system. The highest accumulation event, S2E1, which consists of high rate sub-events separated by brief breaks, features a slow moving low-pressure system that moves across Alaska. The exception to this would seem to be the lengthy S2E3 event, with an upper level cut-

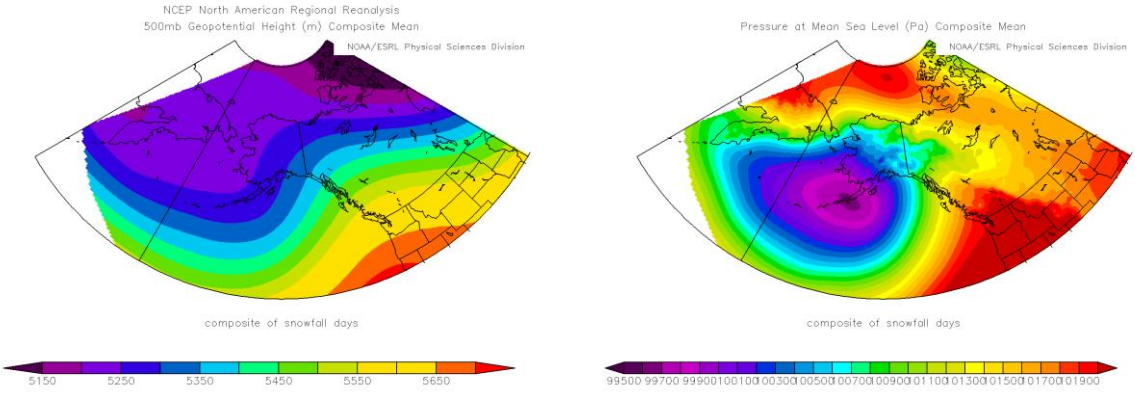

Figure 25: Plots of composite of snowfall days for geopotential height A) 500 mb B) mean sea level pressure

off low and a surface low-pressure system that remain fairly constant in strength, but with significant movement around the Gulf of Alaska. The snowfall occurrences reflect this motion through rapid sub-events with lengthy breaks.

It is possible that conditions leading to immobility tend also to favor low-pressure systems that have weakened and are near dissipating. At this point in a low-pressure system's lifecycle the atmosphere is barotropic: the moist air mass has completely moved into the area, and with no temperature advection or fronts, the atmosphere is stable. This is supported by the hysplit trajectories predominantly showing a lack of mixing and maintaining constant altitudinal difference from one another. This suggests vertical alignment of surface and upper air low-pressure systems. As six trajectories are considered for each time step, each for a different ending altitude over the BBI, the likelihood of moisture delivery from various altitudes can be estimated through variations in their characteristics. In cases with divergence in the horizontal paths of trajectories, it is clear that moisture transport is occurring for some altitudes and not others. Trajectories associated with transport of moisture begin at low altitude over the ocean, often close to the coast. These trajectories then generally show a moderate rise in altitude through the St Elias range and maintain this altitude over the Yukon interior and to the BBI. Some trajectories display brief transit above BBI elevations, suggesting that precipitation is possible from those mechanisms. While it is likely that some of these processes reduce the amount or possibility of precipitation at the BBI, the range of trajectory altitudes indicates that precipitation can occur for a range of atmospheric stability conditions.

For every event, large amounts of moisture are advected towards the NW coast of North America, with the moisture plume generally coming ashore between the south coast of Alaska and central British Columbia. This supports the assumption that large maritime airmasses moving overland in the Gulf of Alaska that are providing the necessary moisture as far inland as the study site. Other potential moisture sources, as mentioned, are either ice covered or too distant. Over the ocean, these plumes of moisture contain a precipitable water content of typically 30 to 40 kg/m^2. As they move over land, the moisture content drops to between approximately one quarter to one half of the original concentration, demonstrating that most is lost to coastal precipitation. As it moves further inland, highly localized moisture which is not resolved by NARR can cause large snowfalls. For example, a significant snowfall occurs during S1E1 when there

is no visible moist airmass present over the BBI (Figure 26A). The reverse is also possible, as a large moist airmass over the area yields only a short and/or low rate event, as seen during S2E3 (Figure 26B).

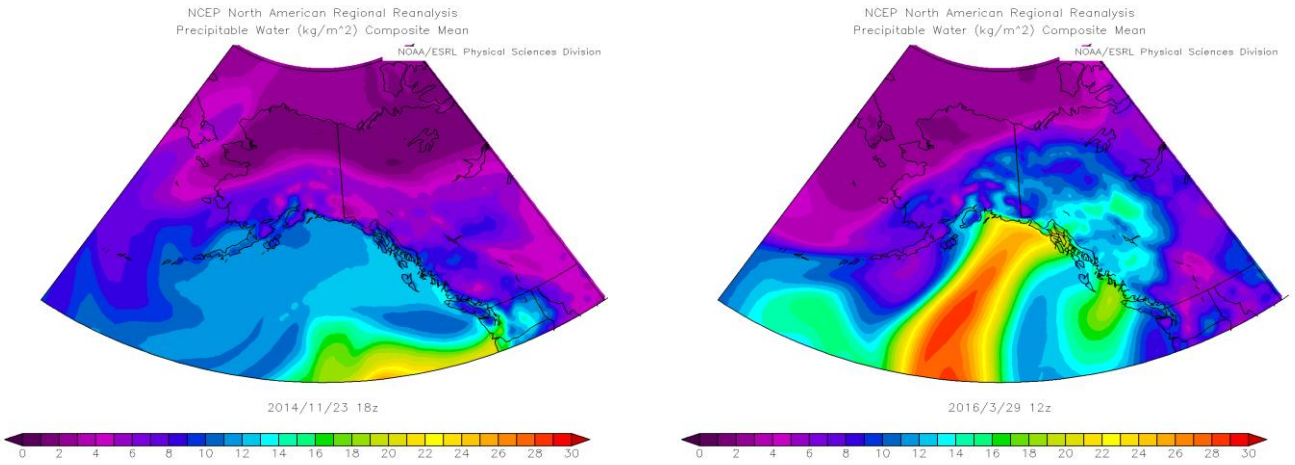

Figure 26: Precipitable water A) S1E1 11/23/2014 and B) S2E3 03/29/2016

During events and sub-events, most air parcel back-trajectories modelled by Hysplit make landfall in key areas on the coast that are linked to the interior by low altitude valleys through the mountains. Small discrepancies between the Hysplit trajectories and the exact paths of lowest altitude are likely due to the scale of the valleys and mountains being on the order of, or less than, the 32 km grid point resolution of NARR (Figure 27). The majority of these entry points for moisture plumes are the outfalls of large river valley systems in the Gulf of Alaska, such as the Alsek river valley, the Lynn canal, the Taku inlet, and the Copper River (Figure 28). There are more possible entry points along the coast of British Columbia as the average elevation of the mountains is lower, however moisture entering the interior must in these instances travel a greater distance to the BBI, and it is likely that such trajectories will not persist in a northerly direction long enough.

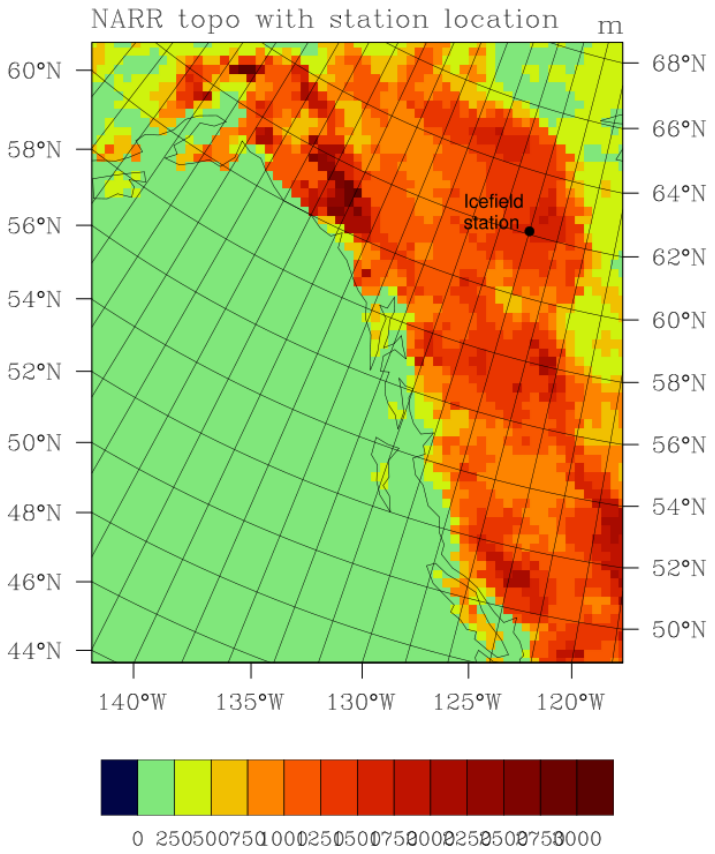

Figure 27: Map of showing resolution of the DEM for 32 km grid NARR reanalysis

Figure 28: Entry points for moist airmasses along the coast

As shown in individual events, most trajectories follow low altitude paths through the mountains and the BBI is the highest topography that they encounter. This is consistent with orographically-enhanced precipitation: air temperature drops with height according to the lapse rate, and colder air can hold less moisture. It stands therefore that large snowfall events will come from airmasses that encounter their greatest elevations at the BBI, and if topography equal or greater in height than the BBI had been encountered, the potential moisture available for snowfall would be reduced. It is likely that the stationary low-pressure centres previously discussed maintain alignment with entry points through the events. Entry points along the coast are discrete and separated from one another by considerable distance. It is likely that some breaks between subsequent sub-events are caused by movement of the low, with the intervening breaks caused by moist air parcels being no longer oriented towards an entry point and instead being intercepted by coastal topography. Snowfall resumes when the interrupted moist air flow finds a new entry point or when a new moist air parcel comes into the old alignment.

Wind direction at the station demonstrates topographic alignment with the up-glacier and down-glacier flow during events. The up-glacier direction is the favourable one for snowfall events with wind direction between 250 and 350 degrees. During events, the wind direction will switch suddenly to roughly opposite to the favourable wind direction: 150 degrees. Interestingly, this is not exactly down glacier flow; 150 degrees is towards

the Nunatak. This corresponds roughly to a NW- SE alignment, similar to the valleys to the immediate south and north of the icefield. The wind directions and speeds at 750 mb are shown to be a controlling factor of winds at the station. In several cases at the BBI it is shown that upper air winds from the west with enough moisture for precipitation potential do not translate to favorable winds at the station, which can be from an entirely different direction. This decoupling of winds aloft and at the glacier surface occurs only when the wind speeds are low. Figure 29 shows that a composite of wind speeds at 750 mb over the BBI on days with STA > 5 cm is approximately double the speed for the entirety of S1 and S2. When the wind speeds aloft are fast enough, they are channeled down and follow the valley axis which also corresponds to the glacier orientation. The channeling can occur by various several mechanisms (Whiteman and Doran, 1999) but in all cases with channeling the wind direction shows a bifurcation with sudden changes depending on the projection of the winds aloft to the valley axis. It has also been shown that winds in Yukon Territory are highly influenced by mountainous terrain, with upper air and surface winds in the Whitehorse Valley following the valley orientation (Pinard, 2008). The consistent alignment of valleys in this area of the Ragged Range may therefore be influencing the upper air winds. Further evidence of the channeling of winds aloft into the valley is the rise in temperature and relative humidity during most events, showing that the precipitating airmass is present at the surface of the icefield. This is supported by the high maximum temperatures for each month (rising up to approximately -4°C) regardless of other temperature statistics for the month.

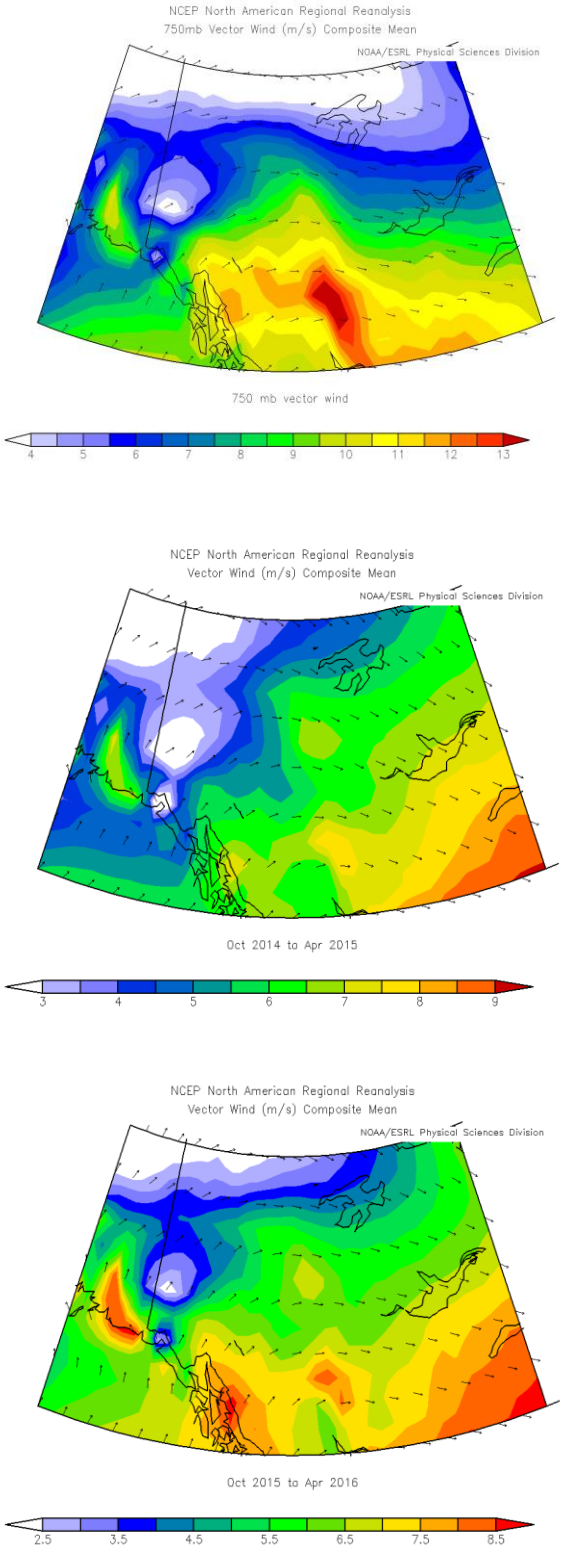

Figure 29: Winds at 750 mb. A) composite of all STA > 5cm days, B) S1, C) S2

The monthly wind roses show strong and frequent winds oriented from the south to the southeast for every month. This is the down-glacier direction. Winds from the west to the northwest, or up-glacier direction, are usually a strong component but can also be almost entirely absent during some months. There are examples of months with frequent and strong up-glacier winds (e.g. Jan S1, Nov S2, Jan S2) with high algorithm totals but without a large event. Two months, November S1 and March S2, exhibit a marked low frequency in the occurrence of up-glacier winds and those that do occur are, on average, weak. Both of these months exhibit the lowest monthly accumulations. Nevertheless, both of these months do have an event, which in both cases happens also to be the only occurrence where the STA was triggered. Dec S1 exhibited frequent up-glacier winds, but they are weak and STA counts are correspondingly low - but does have an event. Some months (Dec S2 and April S2) are characterized by winds other than up-glacier for the most part, but wind speeds are high. December S2 exhibits average STA counts with no event. April S2 exhibits the second highest number of STA counts, almost entirely associated with its two events. As discussed previously, strong winds aloft and at the surface appear to accompany storms and therefore snowfall. It is reasonable, therefore, that the presence of low speed, up-glacier winds is a good indicator of low snowfall, and low frequency of those winds is further associated with low snowfall. The complimentary situation appears not to be valid, however: for example, February of S1 has both strong and frequent up-glacier winds, and only an average snowfall total, and no large event. Most months with at least average frequency and strength of up-glacier winds (Jan, Feb, March and April from S1 and Nov, Jan, Feb from S2), however, exhibit good STA detected snowfall.

Large events show no predictability therefore, as they occur across the spectrum of conditions described above. Smaller events, however, show some predictability based on the frequency of strong up-glacier winds as indicated by the wind roses. There is a range of up-glacier wind directions, commonly being between west-southwest and north-northwest for the various events. This variability appears to be replicated in the monthly wind roses as well. Precipitation variability also appears to be common as inferred from the large departures from normal for AWS stations located along likely trajectories through the Yukon. The variation in frequency by month of large events and of accumulation totals between months is therefore likely normal, and due to the prevalence

of storm tracks that preferentially feed certain areas. Reanalysis plots of anomalies of precipitable water and MSLP plots were examined on a monthly basis, however differences at this scale are too subtle to detect for a relevance to snowfall event timing or frequency. Given the differences in wind direction during the various extreme snowfall events, and the different topographical cross section encountered by the moisture plumes associated with each, it is suggested that interannual variation in the snowpack across the icefield could be a unique signature left by the particular combination of events.

Trujillo et al (2014) classifies snowpack accumulation amount and duration in the Western United States as i) maritime (over 300 cm and fewer than 220 days in the snow accumulation period per year), ii) intermountain (200-300 cm and 220-260 days), and iii) continental (less than 200 cm, more than 260 days). The Brintnell-Bologna Icefield is in the continental regime by these metrics with well under 200 cm of snow and well over 260 days, as snow is possible at all times of year and likely except from June to August. It is, however, only approximately 630 km to the nearest place on the coast, whereas Trujillo et al (2014) finds that mountain ranges in Nevada within 800 km are in the intermountain category. The BBI is separated by only one mountain range from the coast - albeit an extremely tall one - whereas most typical intermountain and continental mountain ranges are several ranges distal from the coast.

In defining snowpack regimes, a key metric is the leading event, defined as the largest single snowfall event in a season. Events are defined in a similar way to this work; a distinct synoptic event lasting up to several days that brings continuous or intermittent snowfall without large breaks. The most commonly used network of data for snowpack regime comparison in the Western United States is the Natural Resources Conservation Service Snowpack Telemetry Network (SNOTEL) which provides long term high-altitude data (Serreze et al, 2001). The unit of measure is the SWE, whereas for this study the unit of measure is an algorithm processed depth measurement. Since relative increase is the parameter of interest for both studies, percentage increases can be calculated and are therefore directly comparable. Some caution should be exercised in interpreting the results, however, as the relation between SWE and depth is modified by density. Density will vary for between individual storms at a given site and certainly vary significantly between maritime and continental sites.

Lute and Abatzoglou (2014) found that for the Western United States, the largest leading events compared to the typical snowfall were maritime in nature (as far as snow-water-equivalent). They found that the greatest number of days with snowfall were at high latitude and high elevation, as this maximized snow versus rain and the path of winter cyclones. The study site location is sufficiently north that most precipitation during the accumulation season will fall as snow. The site is, however, far enough north that it may lay outside the zone of maximum cyclonic activity. For our study, the leading event in S1 provided 23% of the total snowfall amount and for S2, the leading event provided 17%. Lute and Abatzoglou (2014) found that at SNOTEL stations in the interior region, the contribution from leading events was 6-17%. The highest leading event contributions for SNOTEL sites were 13-35% from maritime and intermountain locations. Serreze et al (2001) found the average highest leading events to contribute 10-23%. These correspond to those areas that are directly impacted by Pacific air masses. The leading events for two seasons at the BBI are therefore comparable to the highest values for percentage of leading event observed across the Western United States. In a seminal study that defined the maritime, intermountain, and continental types, Armstrong and Armstrong (1987) found that mean maximum 24-hour snowfall at the aforementioned archtype sites was 91.1 cm, 81.8 cm, and 56.3 cm, respectively. In addition, they determined that the mean number of days per year with more than 30 cm of snow was 10.1, 8.6, and 3.3 respectively. Comparing the absolute magnitude of the large events at the BBI to Armstrong and Armstrong's results then, the BBI is continental. Serreze et al (2001) found that leading event magnitude was seen to increase with maritime proximity but that this was partially due to fewer days where snowfall occurred. The large leading event magnitude at the BBI is also in part due to the relatively small number of snowfall occurences. The few snowfall accumulation days at maritime sites at the mid-latitudes, however, are due to short winters and a large proportion of the year's precipitation falling as rain. At the BBI and other northern latitudes, the few snowfall accumulation days are due to moisture availability. Therefore the BBI accumulation days can not be classified in this context. Serreze et al (2001) also found that in moisture-poor areas, the surrounding topography has a strong influence on the occurrence of events. This is a common finding in recent studies examining extreme snowfalls with

corresponding synoptic conditions and moisture pathways (see for e.g. Swales et al, 2016; Rutz et al, 2014; Faruhk and Yamada, 2014).

7. Conclusions

Large and infrequent snowfall events dominate the accumulation season on the Bologna glacier in the 2014-2015 (S1) and 2015-2016 (S2) accumulation seasons. The events are defined at high temporal resolution, using 15-minute snow depth and hourly wind direction data from an AWS and 3-hour reanalysis plots and back-trajectories. The timing of the beginning, end, and breaks in snowfall for each event was quantified using a snowfall timing algorithm (STA). Snowfall events with a total of at least 20 cm each were analyzed: four such large events were identified in S1 and five in S2. Snowfall events with a total greater than 5 cm were identified individually and used to produce composite reanalysis plots; most large events epitomize the average conditions indicated by these composites. There are, however, notable exceptions; some large events display atypical mechanisms. The end of season snowpack of 1.78 meters in S2 is only slightly larger than the 1.65 meters in S1, but S2 is characterized by greater and more numerous large events and accumulations over 5 cm. Events smaller than 5 cm are not analyzed as they are on spatio-temporal scales too small for consideration, however many likely have synoptic origin as they are a sizeable contribution to the S1 snowpack.

Events were found to depend on specific synoptic and topographical controls, manifested as availability of moisture and wind direction. Wind direction at the AWS predominantly displayed a bifurcation of opposite wind directions corresponding to the NW-SE valley orientation. Large snowfall events occurred exclusively with up-valley winds, always with a westerly component. Changes in wind direction were therefore easily distinguishable and often corresponded exactly to the time of start or end of snowfall. The reanalysis was used to gauge wind speed and direction aloft, with strong winds close to the valley orientation being channeled at the surface. Large fluctuations are observed in monthly variability of wind direction, and while small accumulations are more frequent during months with stronger and more frequent up-valley winds, the occurrence of large events did not appear to be restricted to those months with predominantly favorable wind directions. Moist airmasses resolved at the regional scale were observed to be in transit over the BBI during all occurrences of large snowfall events. Interruptions not due to wind direction change could be attributed to the exit, interruption, or change in direction of these airmasses or lobes within them. The specificity of the conditions necessary for these large snowfall events is evidenced by the

large variation in the intervals between their occurrences, and the variability in their characteristics.

The moisture sources for all events were maritime airmasses making landfall on the Alaska and northern British Columbia coastlines and following low altitude pathways through the high and massive mountains of the St Elias range and across the Yukon territory to the study site. These pathways begin with entry points at the coast, generally major river outlets, which are discrete and separated by significant distances in this area. The constancy in orientation and state of the synoptic mechanism with respect to these entry points and pathways is observed to determine the duration and intermittent nature of events. Some breaks between sub-events are observed to occur when movement of a single low-pressure system causes a moist air mass movement to transition from one entry point to another, with an interruption in snowfall in between.

In this study, the demonstrated controls exerted by topography and moisture trajectories appear to be consistent with those observed in recent studies conducted in the Western United States. Differences in latitude, temperature, storm tracks configurations, and topography, however, should lend caution to any direct comparison. Perhaps the greatest difference between these broad study regions is the proximity of the Saint Elias Mountains whose high and massive mountains and glacierized valleys present topographic controls unlike those anywhere along the remainder of the coast. There are no significant topographic obstacles between the coast range and the Ragged Range, and also to the east of the Mackenzie and Selwyn Mountains as far as the Hudson Bay coastline/Atlantic Ocean. Paradoxically, this simple two range cross section of the continent makes a climate regime classification of the study area difficult, as it is unlike much of the rest of the North American Cordillera to the south.

The enormity of the impact of the leading event as compared to the average event would suggest that the study region lays in a maritime snowfall regime. This is supported by the demonstrably direct and proximate origin of moisture which has not undergone significant transit over topography. The winter air temperature, latitude, and accumulation season length however indicate a more continental classification. Given the very specific conditions that must combine to produce a snowfall event, it is possible that this area, without such a unique filter on the coast, would demonstrate a classic intermountain or continental snowfall accumulation regime, as many more potential

events that are blocked at the coast would make landfall on the icefield. It appears doubtful, however, that this filtering effect is restricting the duration or rate of snowfall for the large events, as they are comparable to the large events in other locations. Therefore negating the effects of the coast range would likely not affect the magnitude of the largest events but increase the number of accumulations at a range of other snowfall event totals, thereby reducing the relative magnitude of the largest events. This would likely approximate the values of a typical intermountain regime. It is proposed then that the traditional maritime, intermountain, and continental labels are ill-suited to such an atypical environment, and it best be described as a highly topographically controlled variant of an intermountain snowfall regime.

References

Anderson, E. R. (2017). Modelling changes in multi-decadal streamflow contributions – Bologna Glacier, Selwyn Mountains, NWT, Canada (M.Sc. Thesis).

Armstrong, R. L., & Armstrong, B. R. (1987). Snow and avalanche climates of the western United States: a comparison of maritime, intermountain and continental conditions. *IAHS Publ*, *162*, 281-294.

Barry, Roger Graham. *Mountain weather and climate*. Psychology Press, 1992.

Benn, D., & Evans, D. J. (2014). *Glaciers and glaciation*. Routledge.

Birkeland, K. W., & Mock, C. J. (1996). Atmospheric circulation patterns associated with heavy snowfall events, Bridger Bowl, Montana, USA. *Mountain Research and Development*, 281-286.

Bitz, C. M., & Battisti, D. S. (1999). Interannual to decadal variability in climate and the glacier mass balance in Washington, western Canada, and Alaska. *Journal of Climate*, *12*(11), 3181-3196.

Bolch, T., Menounos, B., & Wheate, R. (2010). Landsat-based inventory of glaciers in western Canada, 1985–2005. *Remote sensing of Environment*, *114*(1), 127-137.

Brazenec, W. A., & Doesken, N. J. (2005). An evaluation of two ultrasonic snow depth sensors for potential use at automated surface weather observing sites. In *13th Symposium on Meteorological Observations and Instrumentation*.

Brimelow, J. C., & Reuter, G. W. (2005). Transport of atmospheric moisture during three extreme rainfall events over the Mackenzie River basin. *Journal of Hydrometeorology*, *6*(4), 423-440.

Bukovsky, M. S., & Karoly, D. J. (2007). A brief evaluation of precipitation from the North American Regional Reanalysis. *Journal of Hydrometeorology*, *8*(4), 837-846.

Burak, S. A., & Davis, R. E. (2001). Preliminary evaluation of snow accumulation patterns based on storm type, Mammoth Mountain, California, 1996-2001. In *Proc. 69th Annual Meeting, Western Snow Conference, Sun Valley, ID* (pp. 53-58).

Changnon, D., McKee, T. B., & Doesken, N. J. (1993). Annual snowpack patterns across the Rockies: Long-term trends and associated 500-mb synoptic patterns. *Monthly Weather Review*, *121*(3), 633-647.

Campbell Scientific (Canada) Corp. (2012, April 10) SR50A Series Recommended Measurement Interval & Processing. Retrieved from: https://s.campbellsci.com/documents/ca/product-brochures/recommend-measurement-interval-processing-app-note.pdf

DeBeer, C. M., & Sharp, M. J. (2009). Topographic influences on recent changes of very small glaciers in the Monashee Mountains, British Columbia, Canada. *Journal of Glaciology*, *55*(192), 691-700.

Demuth, M. N., & Pietroniro, A. (2003). The impact of climate change on the glaciers of the Canadian Rocky Mountain eastern slopes and implications for water resource-related adaptation in the Canadian prairies. *Geological Survey of Canada Open File*, *4322*, 96.

Demuth, M.N. & Horne, G. (2017). *Decadal-Centenary Glacier Mass Changes and their Variability in Jasper National Park, Alberta, including the Columbia Icefield Region.* Geological Survey of Canada Open File 8229, Ottawa.

Demuth, M. N., & Keller, R. (2006). An assessment of the mass balance of Peyto Glacier (1966–1995) and its relation to recent and past-century climatic variability. *Peyto Glacier: One century of science*, *8*, 83-132.

Demuth, M. N., Pinard, V., Pietroniro, A., Luckman, B. H., Hopkinson, C., Dornes, P., & Comeau, L. (2008). Recent and past-century variations in the glacier resources of the Canadian Rocky Mountains: Nelson River system. *Terra Glacialis*, *11*(248), 27-52.

Demuth, M. N., Wilson, P., & Haggarty, D. (2014). Glaciers of the Ragged Range, Nahanni National Park Reserve, Northwest Territories, Canada. In *Global Land Ice Measurements from Space* (pp. 375-383). Springer Berlin Heidelberg.

Dyurgerov, M. B., & Meier, M. F. (1999). Analysis of winter and summer glacier mass balances. *Geografiska Annaler: Series A, Physical Geography*, *81*(4), 541-554.

Environment and Climate Change Canada. (2016a, June 15). *Canadian Climate Normals.* Retrieved from http://climate.weather.gc.ca/climate_normals/

Environment and Climate Change Canada. (2016b, June 15). *Historical Data.* Retrieved from http://climate.weather.gc.ca/historical_data/search_historic_data_e.html

Fischer, A. P. (2011). The measurement factors in estimating snowfall derived from snow cover surfaces using acoustic snow depth sensors. *Journal of Applied Meteorology and Climatology*, *50*(3), 681-699.

Fisher, D., Wake, C., Kreutz, K., Yalcin, K., Steig, E., Mayewski, P. & Demuth, M. (2004). Stable isotope records from Mount Logan, Eclipse ice cores and nearby Jellybean Lake. Water cycle of the North Pacific over 2000 years and over five vertical kilometres: sudden shifts and tropical connections. *Géographie physique et Quaternaire*, *58*(2-3), 337-352.

Farukh, M. A., & Yamada, T. J. (2014). Synoptic climatology associated with extreme snowfall events in Sapporo city of northern Japan. *Atmospheric Science Letters*, *15*(4), 259-265.

Filhol, S., & Sturm, M. (2015). Snow bedforms: A review, new data, and a formation model. *Journal of Geophysical Research: Earth Surface*, *120*(9), 1645-1669.

Frakes, B., & Yarnal, B. (1997). A procedure for blending manual and correlation-based synoptic classifications. *International Journal of Climatology: A Journal of the Royal Meteorological Society*, *17*(13), 1381-1396.

Goodison, B. E., Metcalfe, J. R., Wilson, R. A., & Jones, K. (1988, April). The Canadian automatic snow depth sensor: a performance update. In *Proceedings of the 56th Annual Western Snow Conference, April* (pp. 19-21).

Halliwell, D. R., & Catto, S. (2003). How and why is aquatic quality changing at Nahanni National Park Reserve, NWT, Canada?. *Environmental monitoring and assessment*, *88*(1), 243-281.

Hodge, S. M., Trabant, D. C., Krimmel, R. M., Heinrichs, T. A., March, R. S., & Josberger, E. G. (1998). Climate variations and changes in mass of three glaciers in western North America. *Journal of Climate*, *11*(9), 2161-2179.

Holdsworth, G., Krouse, H. R., & Nosal, M. (2003). 25 Ice core climate signals from Mount Logan, Yukon AD 1700-1897. *Climate since AD 1500*, 483.

Hudak, D. R., & Young, J. M. C. (2002). Storm climatology of the southern Beaufort Sea. *Atmosphere-Ocean*, *40*(2), 145-158.Hunter, C. (2016). *An evaluation of the North American Regional Reanalysis precipitation fields in a topographically complex domain, British Columbia, Canada* (Doctoral dissertation, University of British Columbia).

Jansson, P., Hock, R., & Schneider, T. (2003). The concept of glacier storage: a review. *Journal of Hydrology*, *282*(1), 116-129.

Judson, A., & Doesken, N. (2000). Density of freshly fallen snow in the central Rocky Mountains. *Bulletin of the American Meteorological Society*, *81*(7), 1577-1587.

Lackmann, G. M., Gyakum, J. R., & Benoit, R. (1998). Moisture transport diagnosis of a wintertime precipitation event in the Mackenzie River Basin. *Monthly Weather Review*, *126*(3), 668-692.

Lackmann, G. M., & Gyakum, J. R. (1999). Heavy cold-season precipitation in the northwestern United States: Synoptic climatology and an analysis of the flood of 17–18 January 1986. *Weather and forecasting*, *14*(5), 687-700.

Lader, R., Bhatt, U. S., Walsh, J. E., Rupp, T. S., & Bieniek, P. A. (2016). Two-meter temperature and precipitation from atmospheric reanalysis evaluated for Alaska. *Journal of Applied Meteorology and Climatology*, *55*(4), 901-922.

Lute, A. C., & Abatzoglou, J. T. (2014). Role of extreme snowfall events in interannual variability of snowfall accumulation in the western United States. *Water Resources Research*, *50*(4), 2874-2888.

Marcus, M. G., & Ragle, R. H. (1970). Snow accumulation in the Icefield Ranges, St. Elias Mountains, Yukon. *Arctic and Alpine Research*, 277-292.

Mesinger, F., DiMego, G., Kalnay, E., Mitchell, K., Shafran, P. C., Ebisuzaki, W., & Ek, M. B. (2006). North American regional reanalysis. *Bulletin of the American Meteorological Society*, *87*(3), 343-360.

Mesquita, M. S., Atkinson, D. E., & Hodges, K. I. (2010). Characteristics and variability of storm tracks in the North Pacific, Bering Sea, and Alaska. *Journal of Climate*, *23*(2), 294-311.

Moore, G. W. K., Alverson, K., & Holdsworth, G. (2003). The impact that elevation has on the ENSO signal in precipitation records from the Gulf of Alaska region. *Climatic Change*, *59*(1-2), 101-121.

Moore, R. D., & Demuth, M. N. (2001). Mass balance and streamflow variability at Place Glacier, Canada, in relation to recent climate fluctuations. *Hydrological Processes*, *15*(18), 3473-3486.

Moore, R. D., Fleming, S. W., Menounos, B., Wheate, R., Fountain, A., Stahl, K. & Jakob, M. (2009). Glacier change in western North America: influences on hydrology, geomorphic hazards and water quality. *Hydrological Processes*, *23*(1), 42-61.

Moore, R. D., & McKendry, I. G. (1996). Spring snowpack anomaly patterns and winter climatic variability, British Columbia, Canada. *Water Resources Research*, *32*(3), 623-632.

Munro, D. S. (2006). Linking the weather to glacier hydrology and mass balance at Peyto glacier. In M.N. Demuth, D.S. Munro, & G.J. Young, (Eds.). *Peyto Glacier: One Century of Science* (pp. 133-176). Saskatoon, Saskatchewan: National Water Research Institute.

National Oceanic and Atmospheric Administration (2016, June 15). *1981-2010 U.S. Climate Normals.* Retrieved from: https://www.noaa.gov/data-access/land-based-station-data/land-based-datasets/climate-normals/1981-2010-normals-data

National Snow and Ice Data Centre (2018, Jan 2). *Sea Ice Index.* Retrieved from: https://nsidc.org/data/seaice_index

Parks Canada (1983). Nahanni National Park Reserve Resource Description and Analysis. *Natural Resource Conservation Section, Parks Canada, Parks Canada, Prairie Region, Winnipeg, Manitoba.*

Pinard, J. P. (2008). *Wind Climate in Yukon Mountainous Terrain*. University of Alberta.

Rodionov, S. N., Bond, N. A., & Overland, J. E. (2007). The Aleutian Low, storm tracks, and winter climate variability in the Bering Sea. *Deep Sea Research Part II: Topical Studies in Oceanography*, *54*(23), 2560-2577.

Rolph, G., Stein, A., and Stunder, B., (2017). Real-time Environmental Applications and Display sYstem: READY. Environmental Modelling & Software, **95**, 210-228,https://doi.org/10.1016/j.envsoft.2017.06.025 .
(http://www.sciencedirect.com/science/article/pii/S1364815217302360)

Rupper, S., Steig, E. J., & Roe, G. (2004). The relationship between snow accumulation at Mt. Logan, Yukon, Canada, and climate variability in the North Pacific. *Journal of Climate*, *17*(24), 4724-4739.

Rutz, J. J., Steenburgh, W. J., & Ralph, F. M. (2014). Climatological characteristics of atmospheric rivers and their inland penetration over the western United States. *Monthly Weather Review*, *142*(2), 905-921.

Ryan, W. A., Doesken, N. J., & Fassnacht, S. R. (2008). Evaluation of ultrasonic snow depth sensors for US snow measurements. *Journal of Atmospheric and Oceanic Technology*, *25*(5), 667-684.

Serreze, M. C., Clark, M. P., & Frei, A. (2001). Characteristics of large snowfall events in the montane western United States as examined using snowpack telemetry (SNOTEL) data. *Water Resources Research*, *37*(3), 675-688.

Shea, J. M., & Marshall, S. J. (2007). Atmospheric flow indices, regional climate, and glacier mass balance in the Canadian Rocky Mountains. *International Journal of Climatology*, *27*(2), 233-247.

Sinclair, K. E., & Marshall, S. J. (2009). Temperature and vapour-trajectory controls on the stable-isotope signal in Canadian Rocky Mountain snowpacks. *Journal of Glaciology*, *55*(191), 485-498.

Sinclair, K. E., Marshall, S. J., & Moran, T. A. (2011). A Lagrangian approach to modelling stable isotopes in precipitation over mountainous terrain. *Hydrological Processes*, *25*(16), 2481-2491.

Spence, C. (2002). Streamflow variability (1965 to 1998) in five Northwest Territories and Nunavut rivers. *Canadian Water Resources Journal*, *27*(2), 135-154.

Stahl, K., Moore, R. D., & Mckendry, I. G. (2006). The role of synoptic-scale circulation in the linkage between large-scale ocean–atmosphere indices and winter surface climate in British Columbia, Canada. *International Journal of Climatology*, *26*(4), 541-560.

Stein, A.F., Draxler, R.R, Rolph, G.D., Stunder, B.J.B., Cohen, M.D., and Ngan, F., (2015). NOAA's HYSPLIT atmospheric transport and dispersion modeling system, Bull. Amer. Meteor. Soc., **96**, 2059-2077, *http://dx.doi.org/10.1175/BAMS-D-14-00110.1*

Swales, D., Alexander, M., & Hughes, M. (2016). Examining moisture pathways and extreme precipitation in the US Intermountain West using self-organizing maps. *Geophysical Research Letters*, *43*(4), 1727-1735.

Trenberth, K. E., & Hurrell, J. W. (1994). Decadal atmosphere-ocean variations in the Pacific. *Climate Dynamics*, *9*(6), 303-319.

Trenberth, K. E., Dai, A., Rasmussen, R. M., & Parsons, D. B. (2003). The changing character of precipitation. *Bulletin of the American Meteorological Society*, *84*(9), 1205-1217.

Trujillo, E., & Molotch, N. P. (2014). Snowpack regimes of the western United States. *Water Resources Research*, *50*(7), 5611-5623.

Walters, R. A., & Meier, M. F. (1989). Variability of glacier mass balances in western North America. *Aspects of climate variability in the Pacific and the Western Americas*, 365-374.

Vaughan, D.G., J.C. Comiso, I. Allison, J. Carrasco, G. Kaser, R. Kwok, P. Mote, T. Murray, F. Paul, J. Ren, E. Rignot, O. Solomina, K. Steffen and T. Zhang, (2013). Observations: Cryosphere. In: Climate Change 2013: The Physical Science Basis. *Contribution of Working Group I to the Fifth Assessment Report of the Intergovernmental Panel on Climate Change* [Stocker, T.F., D. Qin, G.-K. Plattner, M. Tignor, S.K. Allen, J. Boschung, A. Nauels, Y. Xia, V. Bex and P.M. Midgley (eds.)]. Cambridge University Press, Cambridge, United Kingdom and New York, NY, USA.

Whiteman, C. D., & Doran, J. C. (1993). The relationship between overlying synoptic-scale flows and winds within a valley. *Journal of Applied Meteorology*, *32*(11), 1669-1682.

Yarnal, B. (1984). Relationships between synoptic-scale atmospheric circulation and glacier mass balance in South-Western Canada during the International Hydrological Decade, 1965–74. *Journal of Glaciology*, *30*(105), 188-198.

Yarnal, B. (1985). A 500 mb synoptic climatology of pacific north-west coast winters in relation to climatic variability, 1948–1949 to 1977–1978. *International Journal of Climatology*, *5*(3), 237-252.

Zdanowicz, C., Fisher, D., Bourgeois, J., Demuth, M., Zheng, J., Mayewski, P. & Steig, E. J. (2014). Ice cores from the St. Elias Mountains, Yukon, Canada: their significance for climate, atmospheric composition and volcanism in the North Pacific region. *Arctic*, 35-57.